Defence Research and Development Canada
Recherche et développement pour la défense Canada

DRDC Tools for Imagery Exploitation

Final Report

Vincent Labbé
AEREX Avionics Inc.

Defence Research and Development Canada – Valcartier

Contract Report
DRDC Valcartier CR 2013-037
March 2012

Canada

DRDC Tools for Imagery Exploitation

Final Report

Vincent Labbé
AEREX Avionics Inc.

Prepared by:
AEREX Avionics Inc.
324, Saint-Augustin Avenue
Breakeyville (Québec) G0S IEI

Contractor's document number: 2012-92854-1
Contract project manager: Paul Lacasse, 4I8-832-1040
PWGSC contract number: W7701-092854/001/QCL
CSA: François Leduc, Defence scientist, 418-844-4000 x4703

Defence Research and Development Canada – Valcartier

Contract Report
DRDC Valcartier CR 2013-037
March 2012

IMPORTANT INFORMATIVE STATEMENTS

The scientific or technical validity of this contract report is entirely the responsibility of the contractor and the contents do not necessarily have the approval or endorsement of the Department of National Defence of Canada.

Abstract

This document presents a suite of tools implementing the different steps toward automatic change detection on selected satellite images. These tools could be used by an image analyst to facilitate his work, and could also serve for designing an automated detection processing pipeline. This suite of tools is divided into three sets: 1) error prediction and images co-registration, 2) change detection, and 3) target detection. The suite was integrated into Excelis ENVI 4.7/IDL 7.1.1 but was also tested with ENVI 4.8.

Résumé

Ce rapport présente un ensemble d'outils mettant en œuvre les étapes nécessaires à la détection automatique de changements sur un sous-ensemble d'images satellite sélectionnées. Ces outils peuvent assister un analyste dans son travail, ou pourraient être assemblés pour créer une chaîne de traitement automatique. Ces outils sont divisés en trois catégories: 1) prédiction de l'erreur de recalage et recalage d'images, 2) détection de changements et 3) détection de cibles. Cet ensemble d'outils est intégré à Excelis ENVI 4.7/IDL 7.1.1 mais a aussi testé avec ENVI 4.8.

This page intentionally left blank.

Executive summary

DRDC Tools for Imagery Exploitation: Final Report

Vincent Labbé; DRDC Valcartier CR 2013-037; Defence Research and Development Canada – Valcartier; March 2012.

Introduction or background: Accurate change detection is of prime interest for military surveillance operations. Remote sensing is a key source of data for change detection, but this data is challenging in many ways: differences in illumination and angles of view, deformations due to image acquisition, cloud cover, etc. For this reason, remotely sensed images are often exploited by humans assisted of a geographic information system. Limited availability of image analysts leaves a huge amount of data unused. Automated change detection would be ideal for processing this data. However, current state-of-the-art in the domains of automatic image registration and change detection could lead to unsatisfactory results plagued with false alarms. This project proposes to limit automated change detection to data fit for it, thus enabling the exploitation of more data while keeping the performance of automated processing high.

Results: This document presents a suite of tools implementing the different steps toward automatic change detection on selected input images. These tools could be used by an image analyst to facilitate his work, and could also serve for designing an automated detection processing pipeline. This suite of tools is divided into three sets: selection and acquisition of suitable images, change detection on a pair of images and target detection on one image. The suite, called DTIE (DRDC Tools for Imagery Exploitation), was integrated to Excelis ENVI 4.7/IDL 7.1.1 and was also tested on ENVI 4.8

Significance: The suite can be used to evaluate, demonstrate or enhance each of the steps necessary to perform automatic change detection. The tools can also be used for assisted change detection, for supporting image analysts in their work, and to evaluate their need for such tools. One important aspect of this work is the implementation of the SIFT algorithm for images co-registration and target detection. Results with the use of this algorithm will be implemented in another DRDC project related to images co-registration.

Future plans: The suite of imagery exploitation tools could be deployed for evaluation by image analysts, and to identify whether any of them could be used alone with minor modifications. The performance of all the tools presented here could also be enhanced. Especially change detection, which only proposes classical change detection algorithms. The prediction of radiometric normalisation performance was explored, but no satisfactory solution was found. Finally, the suite of tools could be integrated into a single tool performing change detection on a subset of suitable pair of images. The user would have to select a source image and a geographic region of interest. The tool would automatically find suitable images, perform change detection, and present a report to an image analyst for revision. This revision could be used to develop a database of known false alarms to stop reporting them in the future, and a database of good detections, which could be utilized for target detection when change detection is deemed too difficult.

Sommaire

DRDC Tools for Imagery Exploitation: Final Report

Vincent Labbé ; DRDC Valcartier CR 2013-037 ; Recherche et développement pour la défense Canada – Valcartier ; mars 2012.

Introduction ou contexte: La détection de changements est d'un grand intérêt pour les opérations de surveillance militaire. La télédétection est une source privilégiée de données pour la détection de changements, mais le traitement de ces données présente plusieurs défis : différences d'illumination et d'angles de vue, déformation lors de l'acquisition, couvert nuageux, etc. Ainsi, les images satellite sont souvent traitées par un analyste à l'aide d'un système d'information géographique. Cependant, la quantité d'images disponibles est plus grande que la capacité de traitement actuelle. La détection automatique de changements serait la solution idéale, mais les algorithmes actuels de recalage et de détection de changement donnent des résultats imparfaits contenant beaucoup de fausses alarmes. Ce projet propose de limiter la détection de changements automatiques à des données d'entrées appropriées, permettant ainsi le traitement de plus de données en conservant la performance de détection élevée.

Résultats: Ce rapport présente une suite d'outils faisant la démonstration des différentes étapes de traitement permettant la détection automatique de changements sur un ensemble réduit d'images. Ces outils peuvent être utilisés par un analyste pour l'assister dans son travail, et peuvent servir à la mise en œuvre d'une chaîne de détection de changement automatisée. Il y a trois ensembles d'outils : sélection d'images appropriées et planification de missions d'acquisition, détection de changements pour une paire d'images et détection de cibles dans une image. Les outils ont été intégrés à Excelis ENVI 4.7/IDL 7.1.1 et testés sur ENVI 4.8

Importance: La suite d'outils peut servir à évaluer, démontrer et améliorer chacune des étapes requises pour arriver à la détection automatique de changements. Les outils peuvent aussi assister les analystes lors du traitement des images, et évaluer leur besoin pour de tels outils. Un aspect important de ce projet est l'utilisation de l'algorithme SIFT pour le recalage d'images et la détection de cibles. Les résultats obtenus grâce à cet algorithme seront utilisés dans un autre projet de RDDC relié au recalage d'images.

Perspectives: La suite d'outils pour le traitement d'images pourrait être fournie à des analystes pour utilisation et évaluation, et pour identifier quels changements devraient être apportés à certains outils pour les améliorer. Puisque chaque outil met en œuvre des algorithmes classiques, les performances pourraient être augmentées en améliorant ces algorithmes en fonction de situations spécifiques. La prédiction de performance de la normalisation radiométrique ne fait pas partie des outils disponibles et serait un ajout pertinent. Finalement, les outils pourraient être intégrés dans un outil unique faisant la détection de changements automatique sur un ensemble réduit d'images. L'utilisateur aurait à choisir une image source et une région d'intérêt. L'outil trouverait ensuite les images permettant une performance acceptable de détection de changements, ferait la détection de changements sur ces images, et présenterait un rapport à l'analyste pour révision. Les résultats de la révision pourraient servir à développer des bases de données de bonnes détections et de fausses alarmes qui pourraient ensuite servir à la classification des changements détectés, ainsi qu'à la détection de cibles lorsque les conditions ne permettent pas une détection de changements performante.

Table of contents

List of figures

List of tables

Acknowledgements

The author would like to thank Dr. François Leduc for his guidance in the development of the tools and for his continuous testing and commentaries, and Dr. Pierre Lahaie for his supervision and direction through a global vision of the project.

1 Introduction

Accurate change detection is of prime interest for military surveillance operations. Remote sensing is a key source of data for change detection, but this data is challenging in many ways: difference in illumination and angles of view, deformation due to image acquisition, cloud cover, etc. For this reason, remotely sensed images are often exploited by human assisted of a geographic information system. Limited availability of image analysts leaves a huge amount of data unused.

Automated change detection would be ideal for processing large amount of data. However, current state-of-the-art in the domains of automatic image registration and change detection could lead to unsatisfactory results plagued with false alarms. This project proposes to limit automated change detection to data fit for it, thus enabling the exploitation of more data, while keeping the performance of automated processing high.

This document presents a suite of tools implementing the different steps toward automatic change detection on selected input images. These tools could be used by an image analyst to facilitate his work, and could also serve for designing an automated detection processing pipeline. This suite of tools is divided into three sets: selection and acquisition of suitable images, change detection on a pair of images and target detection on one image. The developed tool is named DTIE for DRDC Tools for Imagery Exploitation and the current version is 0.49. The suite was integrated into Excelis ENVI 4.7/IDL 7.1.1 but was also tested with ENVI 4.8

Selection and acquisition of suitable images use the mapping error estimation algorithm developed in the first part of this project [1]. This algorithm was integrated into two tools: estimate mapping error and plan future acquisitions. “Estimate mapping error” uses metadata from two images to identify on which regions change detection can be performed with small registration error. “Plan future acquisition” estimates the acquisition parameters that will result in an image suitable for change detection for a given region.

The “Change detection” tool on a pair of images is implemented in two ways: “single region” change detection and “batch tool” for change detection. Change detection on a single region simply performs extraction of a designated region in a pair of images, registration, change detection and reporting of found changes. The batch tool identifies which images in a lot contain the selected region, and calls the available tools.

Target detection detects a selected pattern in a selected image or region. This tool can be used alone to detect targets; as a replacement when registration is estimated too difficult, or to classify confirmed changes.

The following sections present each image exploitation tool by showing its interface, detailing the underlying algorithm and illustrating its uses with an example.

2 Change Detection Planner

The Change Detection Planner tool contains two functions that are:

1. Estimate Mapping Error: given a pair of images, it finds on which regions change detection could be applied with success;

2. Plan Future Acquisitions: given an image and a region of interest, it estimates the acquisition parameters (viewpoint) of a second image suitable for change detection operations.

Figure 1 shows the two elements of the Change Detection Planner tool that were added to the ENVI software menu. The following two sections present their functionalities in detail. Both elements use the estimating mapping error function, which was developed in the first phase of this project [1]. Both algorithms require a digital elevation model (DEM) of the selected region.

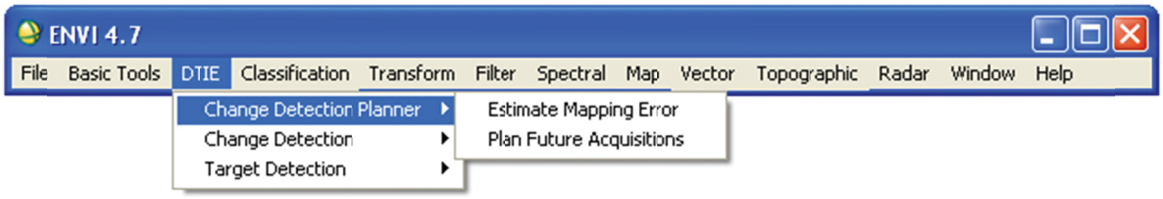

Figure 1: Change Detection Planner menu in ENVI

2.1 Estimate Mapping Error

Estimate Mapping Error identifies, given two viewpoints, on which part of an image (or region) change detection could be applied with a limited number of false alarms. To accomplish this, the whole image is separated into smaller tiles and the mapping error is estimated for each tile. The results are presented to the user as a coloured image of green, yellow and red regions, showing small, average and high estimated co-registration errors respectively. This allows the user to know if a pair of images is suitable for change detection operations of a given Region of Interest (ROI).

2.1.1 Usage

Upon selecting Estimate Mapping Error from the DTIE menu, the user is asked to select a reference image (also called first image), as shown in Figure 2. This image is the base image, i.e. the starting image from which one would like to detect changes by comparing it to another image.

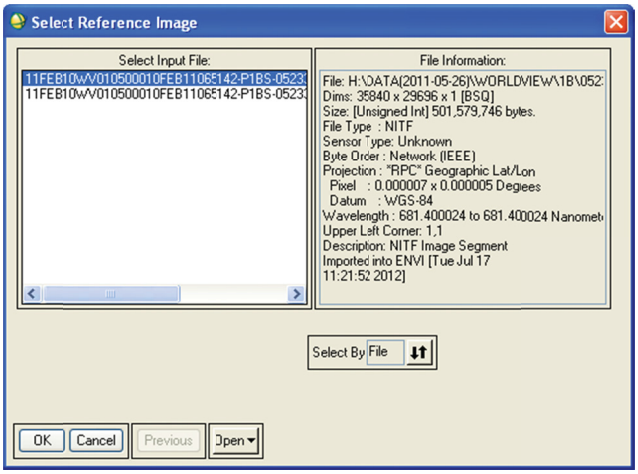

Figure 2: Select Reference Image dialog box

Next, two options are presented to the user, as shown in Figure 3. The user can select a target image, from which the satellite viewpoint will be extracted, or the user can manually enter the desired viewpoint relative to the reference image (called attitude offset in the dialog).

Figure 3: Select Target dialog box

If Target Image is selected, the Select Target image dialog box is presented to the user (see Figure 4).

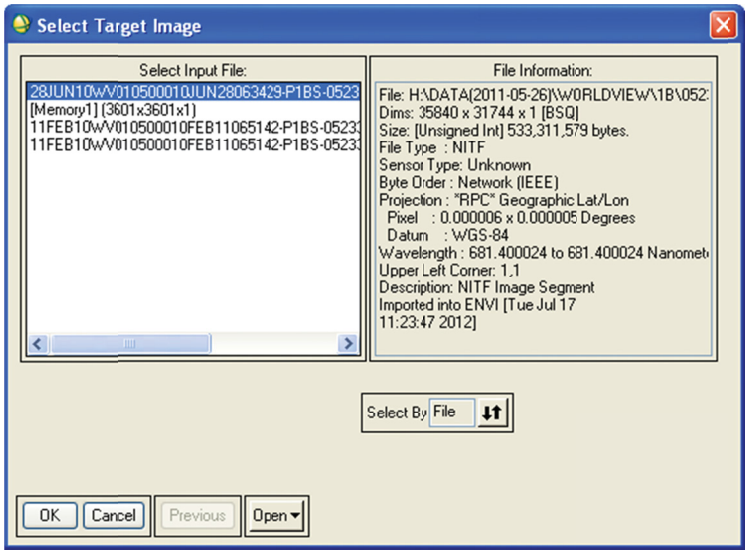

Figure 4: Select Target Image dialog box

If Attitude Offset is selected, the user enters azimuth and zenith offsets that will be added to the reference image viewpoint (see Figure 5).

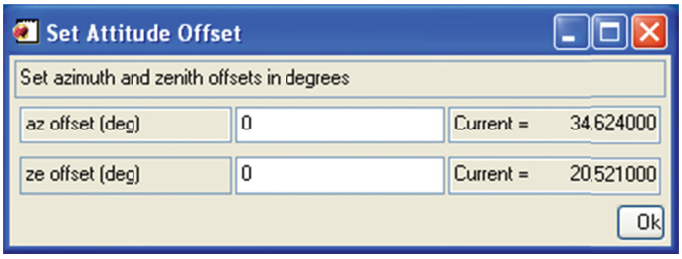

Figure 5: Set Attitude Offset dialog box

After the second viewpoint is set, the tool then proceeds to estimate mapping error.

2.1.2 Algorithm

The first step is to get digital elevation data corresponding to the ROI. The algorithm finds the right DEM from the DEM directory, extracts and realigns DEM data to match the region of interest and its relative orientation respecting the reference image. The DEM data is then divided into tiles, and a mapping error is calculated for each tile. If a second image is selected by the user, a second viewpoint is available and we can determinate which points are present in both images.

Note that the change detection algorithm, presented in section 3.1.2, uses the ancillary geographic coordinates available with WorldView test imagery to perform an approximate warping, before proceeding with the co-registration algorithm. This transformation does not have any impact on relief-induced deformations that increase mapping error (which is the error estimated by the current tool).

2.1.3 Example result

The result presented in figure 6 was generated using a reference image and an attitude offset of five degrees in zenith. Figure 6 shows the estimated mapping error represented as tiles of color overlaid on the reference image. One can see that a difference of five degrees in zenith results in high mapping error only on tiles situated in mountainous regions.

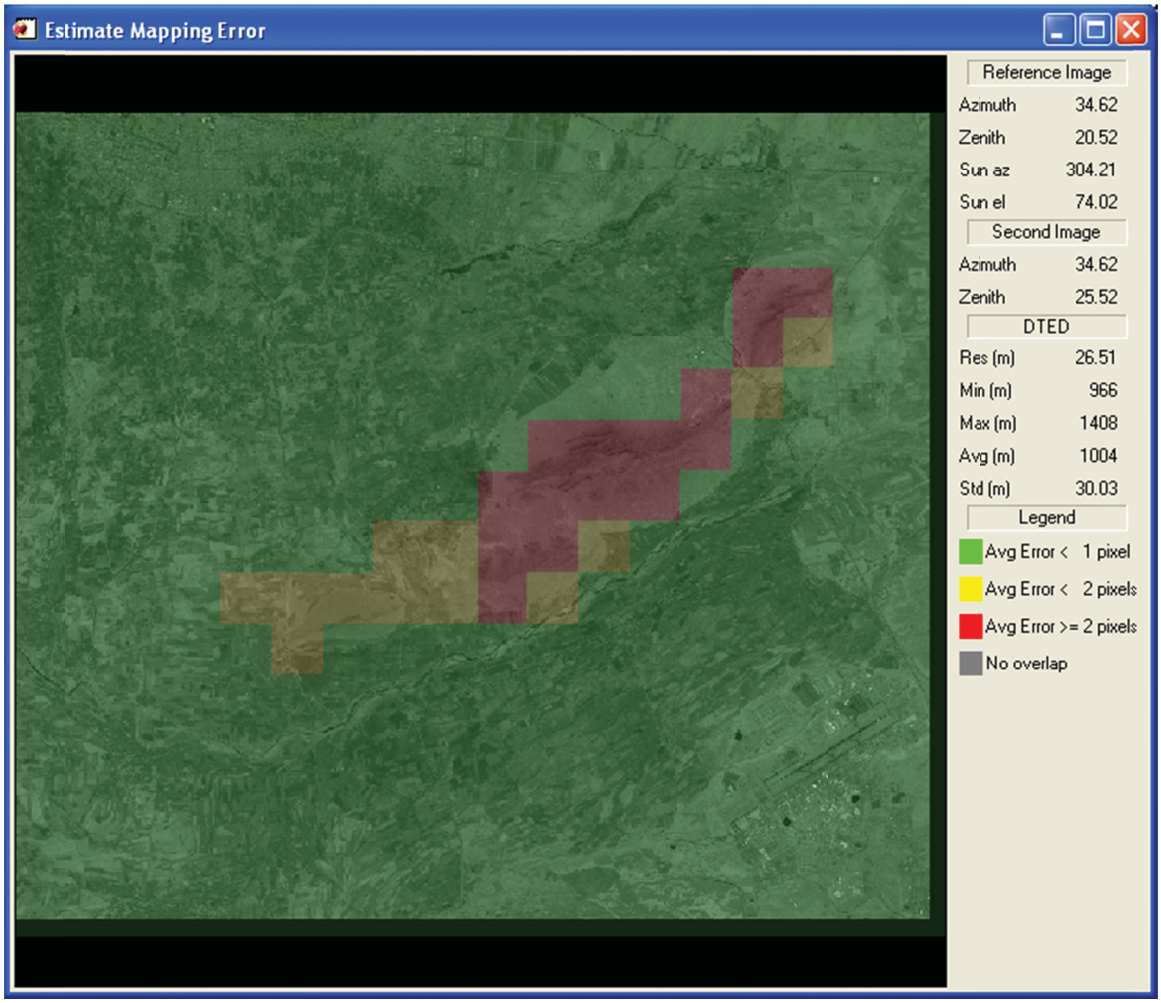

Figure 6: Estimate Mapping Error – Example result

2.2 Plan Future Acquisitions

The "Plan Future Acquisitions" function generates, for a given region, a report presenting the acquisition conditions suitable for a second image for change detection operations.

2.2.1 Usage

The user selects an input image and a region in that image by clicking the spatial subset button (Figure 7). A region can be defined by a polygon using the ENVI ROI tool or by a vector file.

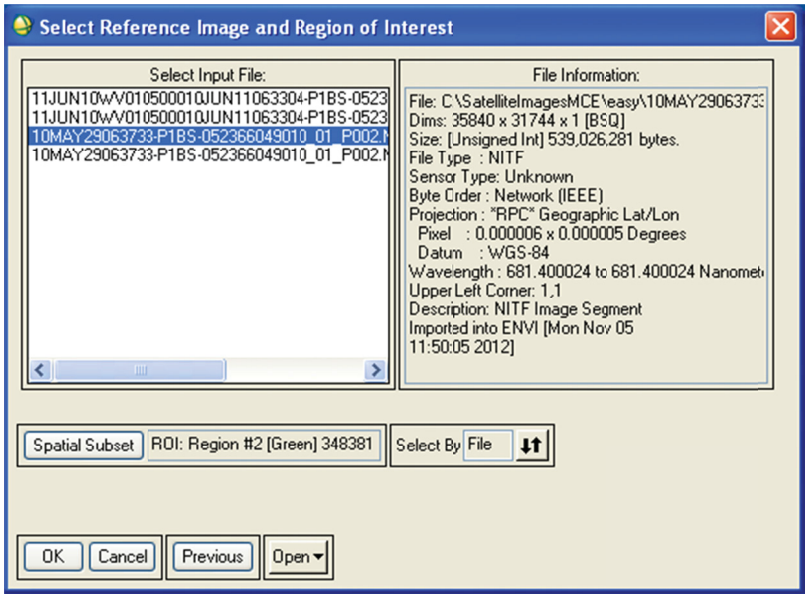

Figure 7: Select Reference Image and Region of Interest dialog box

Afterwards, the mapping error is estimated for a range of viewpoints and the results are recorded in a Microsoft Word report.

2.2.2 Algorithm

The algorithm begins by retrieving the DEM data (corresponding to the selected region) and the sensor viewpoint (from the metadata of the selected image). It then performs a coarse estimation of the mapping error in increments of one degree at a time, for azimuth and zenith, until the error reaches two pixels. The azimuth and zenith ranges are each split into 20 increments, for which a finer mapping error estimation is calculated. Finally, a Microsoft Word report is created using the extracted metadata and the calculated mapping error. The next section presents the main results.

2.2.3 Example result

The Plan Future Acquisition function generates a Microsoft Word report. This report is meant to be a draft that will be edited by the analyst. A complete example of the generated report is presented in Annex C. This section discusses the main elements of this report.

The report presents the reference image and the selected region of interest, shows the topography of that region, and gives the range of acquisition parameters deemed valid for acquiring an image suitable for change detection.

The most significant result of this function is presented in Figure 8. This figure shows the mapping error resulting from a difference in satellite elevation and zenith. The original viewpoint (from the image selected by the user) is at the center of the figure. Increasing differences in azimuth and zenith result in greater mapping error. The lines show the limits for mapping errors of 0.5, 1, 1.5 and 2 pixels. The region colored in light green is considered ideal for change detection. The region in darker green could be considered acceptable. Crosses correspond to the points for which mapping error was estimated.

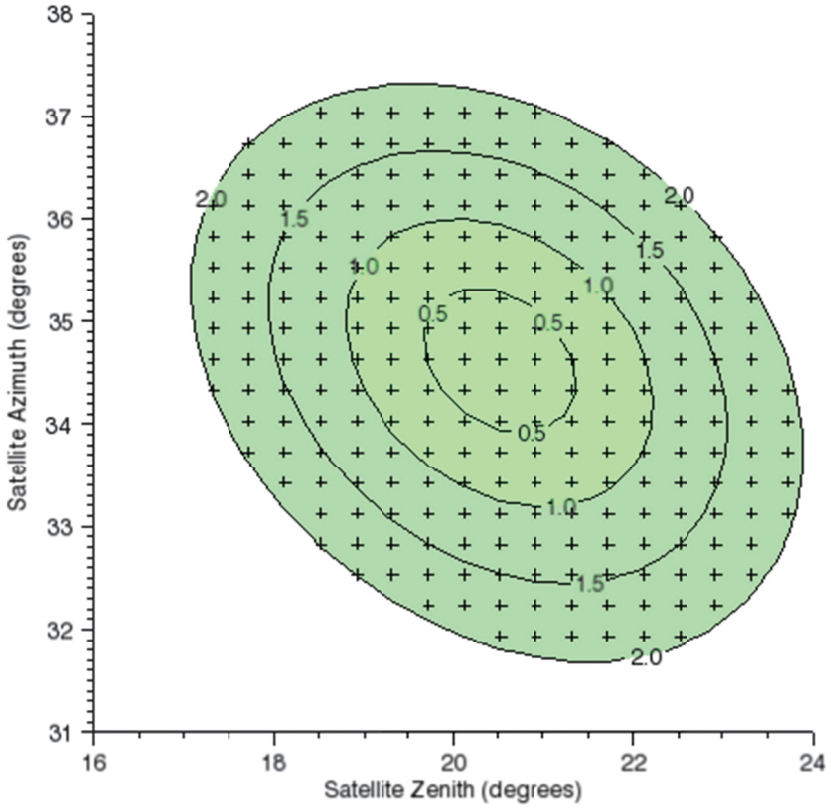

Figure 8: Valid satellite attitudes for image acquisition

3 Change Detection

The Change detection operation identifies generic changes by comparing two images of the same area acquired at different times. The change detection module contains two tools that are: a standard change detection algorithm and a batch tool to assist in selecting candidate images for change detection.

These two tools are accessible through the Change Detection button under the DTIE main menu, as shown in Figure 9. Each tool is presented in detail in the following sections.

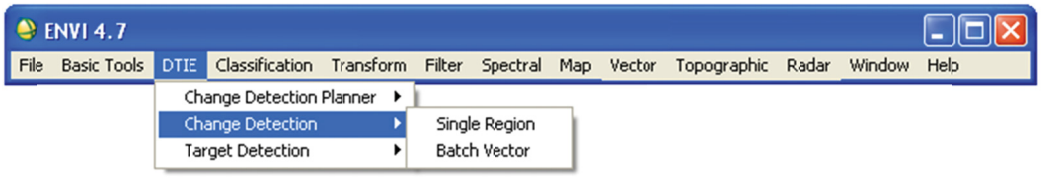

Figure 9: Change Detection menu in ENVI

3.1 Single Region

The "Single Region" tool is used to perform change detection on a pair of images for a specific region.

3.1.1 Usage

Upon selecting the Single Region menu item shown in Figure 9, the user is presented with the Select Reference Image and Region of Interest dialog box, shown in Figure 10 below. The user can select an image already opened in ENVI in the Select Input File control, or open a new image file by selecting the Open button (arrow number 1 in Figure 10). Then the user selects a region of interest, on which change detection will be performed, by pressing the Spatial Subset button (arrow number 2).

The "Select Spatial Subset" dialog box (shown in Figure 11) allows specifying a subset of the reference image by choosing an already defined Region of Interest (ROI) or a vector file (which specifies a region of interest in geographical coordinates). Figure 12 shows the dialog displayed if the ROI is specified by choosing an existing ROI or vector file. Figure 13 shows the resulting Select Reference Image and Region of Interest dialog box.

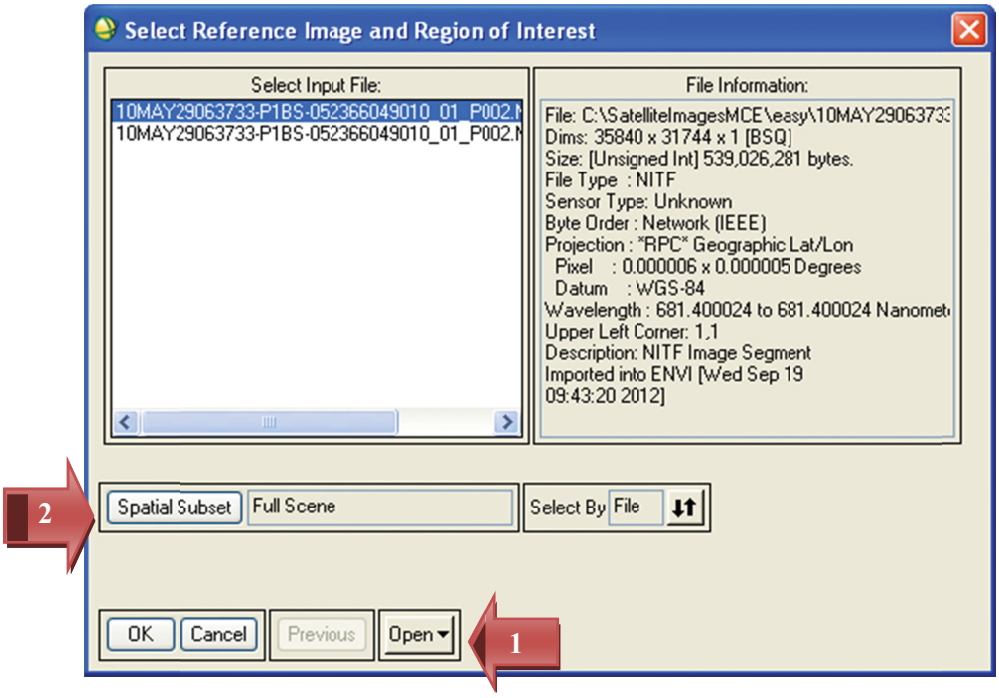

Figure 10: Select Reference Image and Region of Interest dialog box

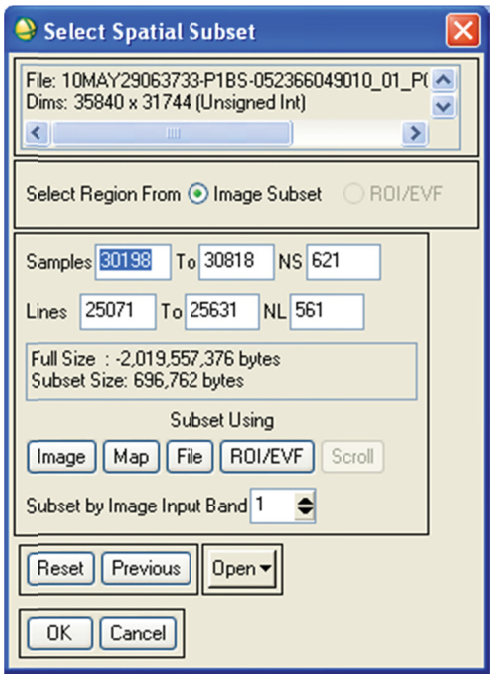

Figure 11: Select Spatial Subset dialog box

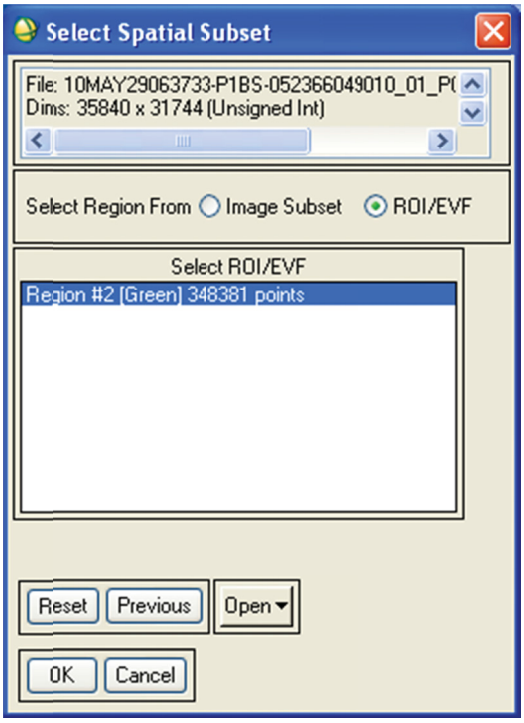

Figure 12: Select Spatial Subset ROI dialog box

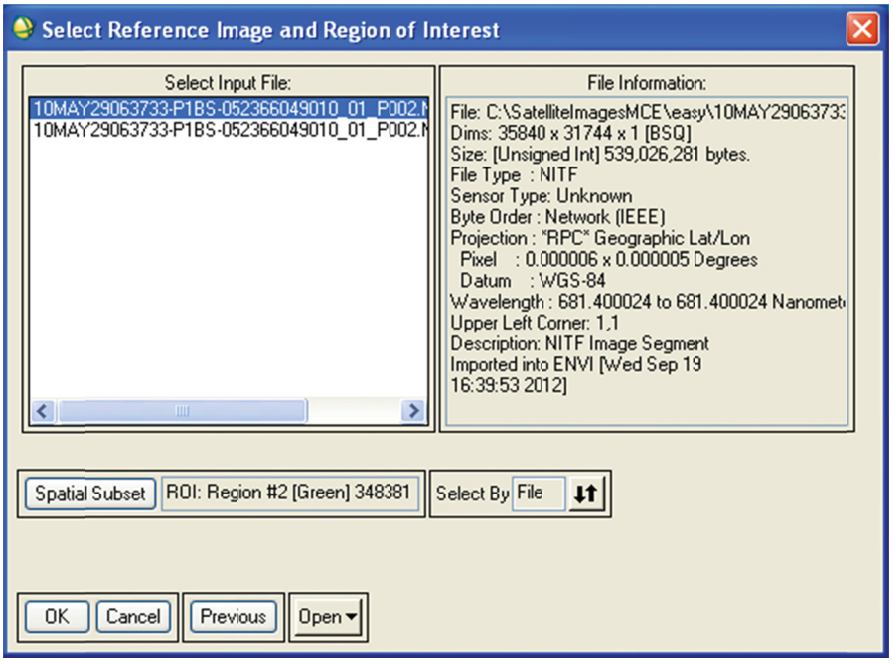

Figure 13: Resulting Select Reference Image and Region of Interest dialog box

After having pressed the OK button to confirm selection of the reference image and its subset, the user has to select the sensed image (also called second image), which will be compared to the reference image (or first image) for change detection. The Select Sensed Image dialog box is

shown in Figure 14. This dialog box is similar to the Select Reference Image and Region of Interest dialog box, without the Spatial Subset button because the region of the sensed image corresponding to the selected region of interest in the reference image will be extracted by the tool.

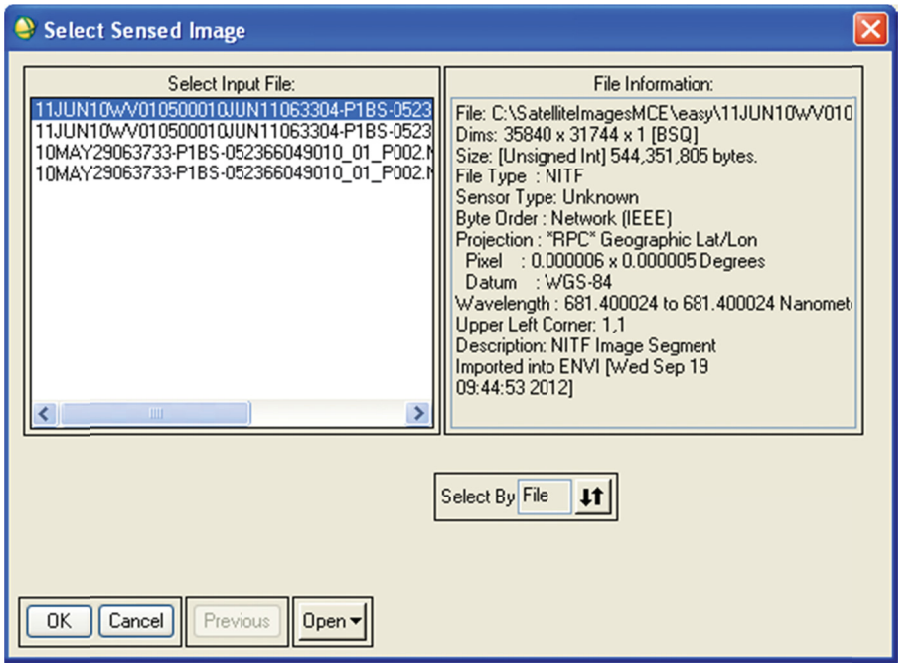

Figure 14: Select Sensed Image dialog box

3.1.2 Algorithm

Since the objective of this project was not to create a new change detection algorithm for a specific case, but rather to select suitable input images, a classical change detection processing chain has been implemented. This chain follows these steps:

1. **Registration**: transform the sensed image into the coordinate system of the reference image (images are then in the same spatial frame);

2. **Radiometric adjustment**: normalise the sensed image pixel intensities to compensate for differences in illumination (image are then in the same radiometric frame);

3. **Change metric**: calculate a degree of change for each pixel in the region of interest;

4. **Thresholding**: apply a threshold on the degree of change to identify changes.

Change metric (step 3) and Thresholding (step 4) are often performed in a single step (see [2] for examples of change detection algorithms). Separating them into two distinct steps allows trying different combinations. For example, a new thresholding algorithm could be evaluated with different change metric algorithms to find the best combination.

The following subsections detail each step of the change detection processing chain.

3.1.2.1 Registration

Image registration is the alignment of two or more images into the same coordinate system. In practice, if two images are to be compared, data from one image (sensed image or second image) is transformed into the coordinate system of the other image (reference image or first image).

Image co-registration methods have been extensively reviewed by Brown [3], Zitova and Flusser [4], and more recently by Wyawahare et al.[5]. Existing image co-registration techniques fit into a generic frame, where an image transformation model is estimated from sets of control points.

The generic image co-registration process can be divided into three steps:

1. Control points selection and matching;

2. Control points mapping estimation; and

3. Image transformation.

Control points selection and matching consists in selecting, in the sensed image and the reference image, 2D points referring to the same 3D reality. Mapping estimation uses these control points to estimate a transformation from 2D points in the sensed image to 2D points in the reference image. Image transformation applies the mapping to transform the content of the sensed image into the coordinate system of the reference image.

Control points selection

Control points selection has to be automated since this project aims at developing an automated change detection processing chain. A small literature review has shown that there are many control point detectors [4, 6-8]. Selections of point detectors were implemented in IDL (Interactive Data Language) in: Harris corner detector [9], Noble version of Harris corner detector [10], SIFT (Scale-invariant feature transform) [11], Difference of Gaussian [11], Laplacian of Gaussian [12], Harris-Laplacian [13], Hessian-Laplacian [13], and FAST [14]. **Error! Reference source not found.** Figure 15 shows the results obtained by applying these control point detectors on a test image.

It can be seen from figure 15 **Error! Reference source not found.**that corner detectors (Harris and Harris-Noble) are very good at detecting all the corners with precision. The other interest point detectors give less intuitive results, where an interest point can be located in a uniform black area. Points reported by SIFT tend to be corners. SIFT was chosen because it demonstrated overall best performance on informal tests on pairs of test images (from the test dataset presented in Annex A). Also, SIFT points have the desirable properties of being, at least to some extent, invariable to scale, and to a minor extent, invariable to rotation.

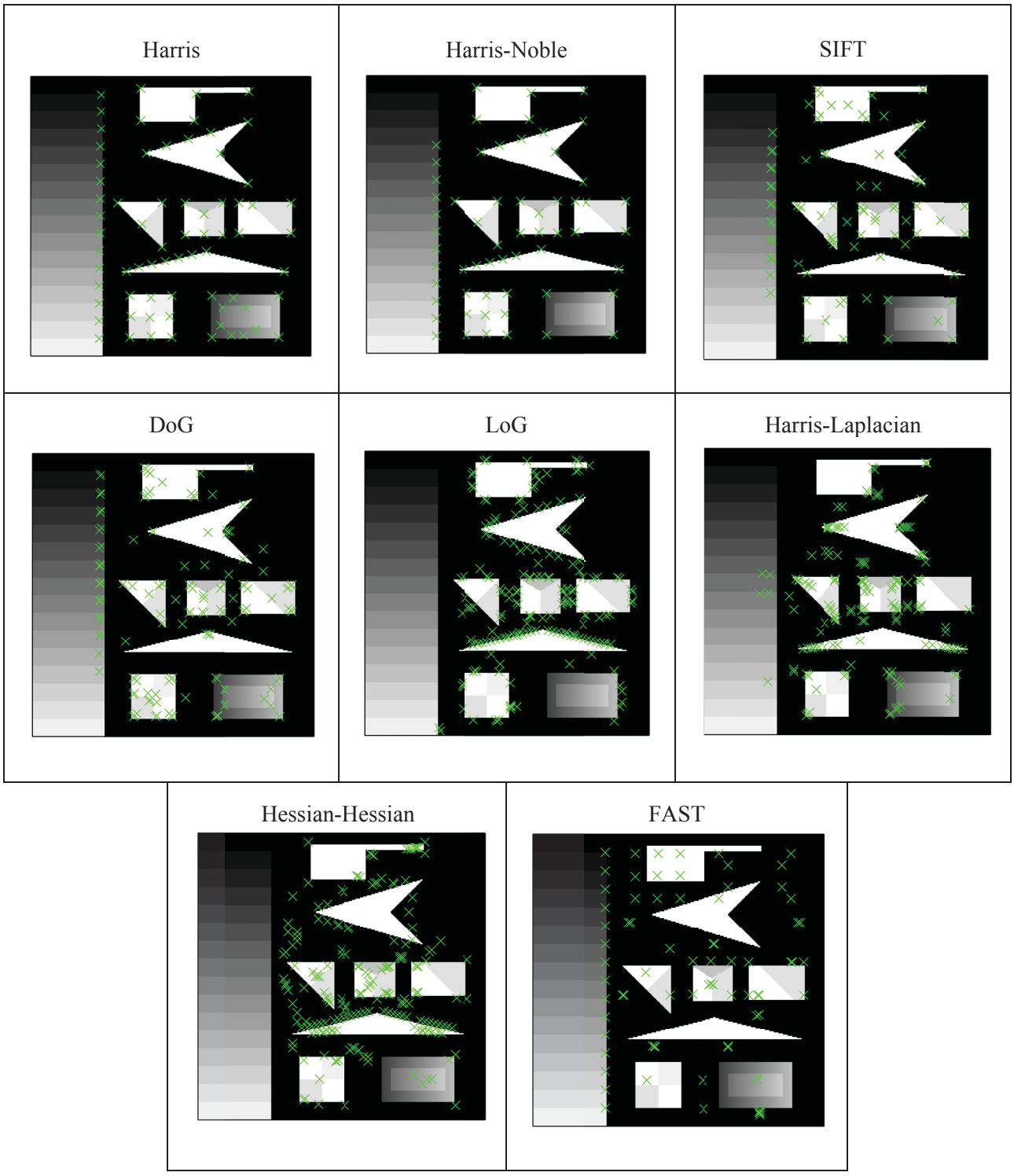

Figure 15: Interest point detectors test results

Control points matching

SIFT provides, for each control point found, a descriptor that can be used to perform matching [11]. The method used here for putative matching is the one proposed by Lowe [11]. The best match for each point is found by finding the point with the minimum Euclidean distance in the feature space. A ratio of distances is used as a threshold. Please refer to the original paper [11] for more details.

Control points mapping estimation

The matching of control points done in the previous step will result in correct and incorrect pairs of points (an incorrect pair of points being two points not pointing to the same real world element). To get rid of the incorrect pairs of points, mapping estimation is realised by using the Random Sample Consensus (RANSAC) algorithm [15]. This algorithm finds, given a model, the parameters explaining the greatest number of points. This allows ignoring outliers during model parameter estimation.

In the first part of this project, a number of mapping algorithms were evaluated [1]: polynomial mapping (first and second order), projective mapping, piecewise linear mapping and polynomial mapping using image partitioning. Piecewise linear mapping is not based on a model and cannot be used with RANSAC. Polynomial mapping with image partitioning requires a lot of points (because many points are needed for each partition) and is not practical in an operating context. Of the three global mapping algorithms (first and second order polynomial, and projective), first order polynomial clearly underperforms. Projective mapping was chosen instead of second order polynomial mapping because it needs less points to evaluate a model (only four) and second order polynomial mapping can infer strange mappings in the regions between control points. For these reasons, the model provided to RANSAC is projective mapping.

Once RANSAC has found the set of four points explaining the greatest number of matching points, all the non-outlier points are used to estimate a projective mapping by the least-square error minimisation.

Image transformation

The coordinate transformation model found in the previous step (Control points mapping estimation) is used to transform the sensed image into the coordinates of the reference image. For each point of the reference image, the corresponding point in the sensed image is found, and placed in the transformed image through bilinear interpolation.

3.1.2.2 Radiometric adjustment

Once spatially registered, the two images selected for change detection need to be radiometrically adjusted. This intends to reduce false alarms by compensating for irrelevant changes like difference in illumination.

Three radiometric adjustment algorithms are available in DTIE: min-max, normalisation and histogram matching. They are presented in the following subsections by equations describing the

transformation from sensed image to normalised sensed image. More details on radiometric adjustments can be found in [16].

Definitions

The following definitions are used in the equations describing the radiometric adjustments:

Ref : reference image
Im : sensed image
Im': adjusted sensed image
x,y: pixel coordinates
Z(x,y): pixel value at coordinates *x, y*

Min-max

The "Min-max" algorithm simply maps the minimum value of the sensed image to the minimum value of the reference image, the maximum value of the sensed image to the maximum value of the reference image, and performs linear interpolation between the minimum and maximum to map the remaining values. Equation (1) describes the "Min-max" transformation.

$$Im'(x,y) = \max(Ref)\frac{Im(x,y) - \min(Im)}{\max(Im) - \min(Im)} + \min(Ref) \quad (1)$$

Normalisation

The "Normalisation" algorithm transforms the sensed image in order to match the mean and standard deviation of the reference image. Equation (2) describes the "Normalisation" transformation.

$$Im'(x,y) = \frac{\sigma(Ref)}{\sigma(Im)}\big(Im(x,y) - \mu(Im)\big) + \mu(Ref) \quad (2)$$

Histogram Matching

The "Histogram Matching" algorithm transforms the sensed image in order to match the histogram of the reference image. Because this algorithm is implemented by using the Cumulative Distribution (CDF) function, it is also called CDF stretch [16]. CDF stretch is described in equation (3). Histogram matching is used in our implementation of change detection.

$$Im'(x,y) = CDF_{Ref}^{-1}(CDF(Im(x,y))) \quad (3)$$

3.1.2.3 Change metric

A change metric algorithm outputs, for each pixel, a value proportional to the estimated degree of change. Four change metric algorithms were implemented in DTIE: simple differencing, geo-pixel, FL Ratio and shading model. The following sections detail each of these algorithms.

Simple differencing

Simple difference is the classical image subtraction technique. Each pixel of the co-registered and radiometrically adjusted sensed image is subtracted to the reference image. This technique is very fast and intuitive but also very sensitive to registration errors and radiometric adjustments errors. Equation (4) describes the simple differencing metric.

$$D(x,y) = Ref(x,y) - Im'(x,y) \tag{4}$$

Geo-pixel technique

The Geo-pixel technique [17] was developed to overcome problems associated with sensitivity to noise. This methods compares statistics from two corresponding neighbourhoods (one from the reference image and the other from the sensed image) using a likelihood ratio.

For a neighbourhood *N* of size *s*

$$N(x,y) = \{Z(i,j) | x - s \leq i \leq x + s, y - s \leq j \leq y + s\} \tag{5}$$

The likelihood ratio is computed using the mean and variance of each region

$$L(x,y) = \frac{\left[\frac{(\sigma^2(N_{Ref}) + \sigma^2(N_{Im}))^2}{2} + \left(\frac{\mu(N_{Ref}) - \mu(N_{Im})}{2}\right)^2\right]^2}{\sigma^2(N_{Ref})\sigma^2(N_{Im})} \tag{6}$$

If the likelihood ratio is greater than a specified threshold, this indicates that the two regions surrounding the pixel of interest do not originate from the same distribution.

FL Ratio

The FL Ratio metric, named after Dr. François Leduc from DRDC Valcartier who came with the idea, hypotheses that the degree of change does not only depend on the difference between the two values of a pixel, but also on the underlying values. The intuition behind this idea is that a change in value from 1 to 2 is more significant than a change from 1000 to 1001. This resulted in a change metric where the difference between two values is normalised by the greatest value

$$D(x,y) = \frac{|Ref(x,y) - Im'(x,y)|}{\max(Ref(x,y), Im'(x,y))} * 100 \tag{7}$$

This technique is sensitive to change on low intensity pixels, and less sensitive to pixels with high intensity. Dividing the difference between the two pixels by their maximum value confines the

ratio to values between 0 and 1. The direction of change that would otherwise have been indicated by the sign is lost, but this information is irrelevant for our application. The FL Ratio metric does not require radiometric adjustment but should only be used on images in a similar dynamic range.

Shading model

The Shading Model technique [2, 17] supposes that a specific pixel intensity can be modeled as the product of the illumination of the scene and the surface reflectance. If we assume that surface reflectance stays the same for the pair of images being processed (it it reasonable since they are images of the same scene, except for the changes), then we are left with the illumination components only. Since illumination is supposed uniform, or at least regionally uniform, one can compare two neighbourhoods for change by calculating the ratios of pixel intensities in that neighbourhood and look for non-uniform distributions. A high variance would be a sign of non-uniform distribution.

For a neighbourhood *N* of size *s*

$$N(x,y) = \{Z(i,j) | x - s \leq i \leq x + s, y - s \leq j \leq y + s\} \quad (8)$$

To calculate the change metric for each neighbourhood, one simply needs to calculate the variance of the intensity ratio.

$$L(x,y) = \sigma^2\left(\frac{N_{Ref}}{N_{Im}}\right) \quad (9)$$

This technique is invariant to uniform changes in illumination and sensitive to non-uniform changes on intensities in a neighbourhood.

Discussion

The four change metrics methodologies presented in this section have been implemented in DTIE. Although geo-pixel and shading model performed well on images with large and non-uniform differences in illumination, they were discarded due to their lesser sensitivity to small changes. Two metrics were kept: simple differencing and FL Ratio. Simple differencing provides intuitive results and false alarms can be mitigated later in the processing chain. Because its results are limited to the [0,100] range, FL Ratio is an adequate metric to use with a soft threshold, i.e. many discrete degrees of change are reported to the user. Section 3.1.3 presents results obtained with these two metrics.

3.1.2.4 Mitigation of false detection

In order to reduce false alarms, it was proposed by Elgammal, Harwood and Davis [18] to compare a pixel not only to its corresponding pixel, but also to the other pixels of the neighbourhood, and to take the smallest difference. This accounts for small registration errors, small movements and shadows.

Let T_1 and T_2 be two registered images, A_0 the value of a pixel in T_1, B the value of the corresponding pixel in T_2, and $B_1$to $B_n$the values of the pixels in the neighbourhood *N* of B. The change metric in $A_0$is then (if using simple difference as a metric):

$$D(A_0, B) = \min_{y \in N(B)} (|A_0 - B_y|) \quad (10)$$

This is illustrated in Figure 16. The pixel $A_0$is compared to every pixel in the neighbourhood of pixel B. Comparison is done by calculating the change metric between A_0 and the selected pixel of the neighbourhood.

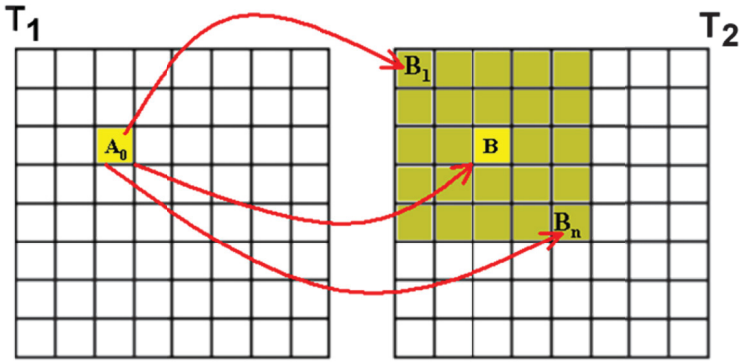

Figure 16: False detection mitigation. Source: [19]

3.1.2.5 Thresholding

A threshold must be applied on the change metric to get detections. This threshold can be a global hard threshold or a soft threshold. A hard threshold is a two-class classifier: below the threshold or above the threshold. A soft threshold results in a multi-class image (for example a nine-class image for nine degrees of change). A soft threshold allows showing to the user a level of confidence on the reported detection.

Since the change metric reported by simple differencing can have any value, thresholding is often implemented as a distance of two or three standard deviations from the mean. This assumes that a number of pixels have changed, whatever the magnitude of change. On the other hand, FL Ratio results in change metrics between 0 and 100, which allows defining absolute thresholds. It is important for the analyst to keep that in mind when interpreting detections reported through simple differencing: the largest difference is reported as change.

3.1.3 Example results

This section presents results from change detection for an easy case. Two WorldView 1 images, acquired at different dates and from different viewpoints, are used, as detailed in Table 1.

Table 1: Image pair metadata for single region change detection example

Reference image - 10MAY29063733-P1BS-052366049010_01_P002.NTF						
Azimuth (degrees)	**Zenith (degrees)**	**GSD (cm)**	**Sun Azimuth (degrees)**	**Sun Elevation (degrees)**	**Date**	**Time**
34.62	20.52	0.55	304.21	74.02	2010-05-29	06:37:33
Sensed image - 11JUN10WV010500010JUN11063304-P1BS-052370310010_01_P002.NTF						
Azimuth (degrees)	**Zenith (degrees)**	**GSD (cm)**	**Sun Azimuth (degrees)**	**Sun Elevation (degrees)**	**Date**	**Time**
66.88	24.07	0.58	296.60	73.66	2010-06-11	06:33:34

Figure 17 presents the graphical interface showing the detection results to the user. Upon clicking on the left mouse button, the user can navigate from Reference image, Sensed image (registered to reference image), and Multiview image. Multiview image shows reference image in the red band and sensed image in the green band. This allows to easily view the differences between the two images. In fact, this 2-color multiview is the simplest change detection method which does not require any computation algorithm.

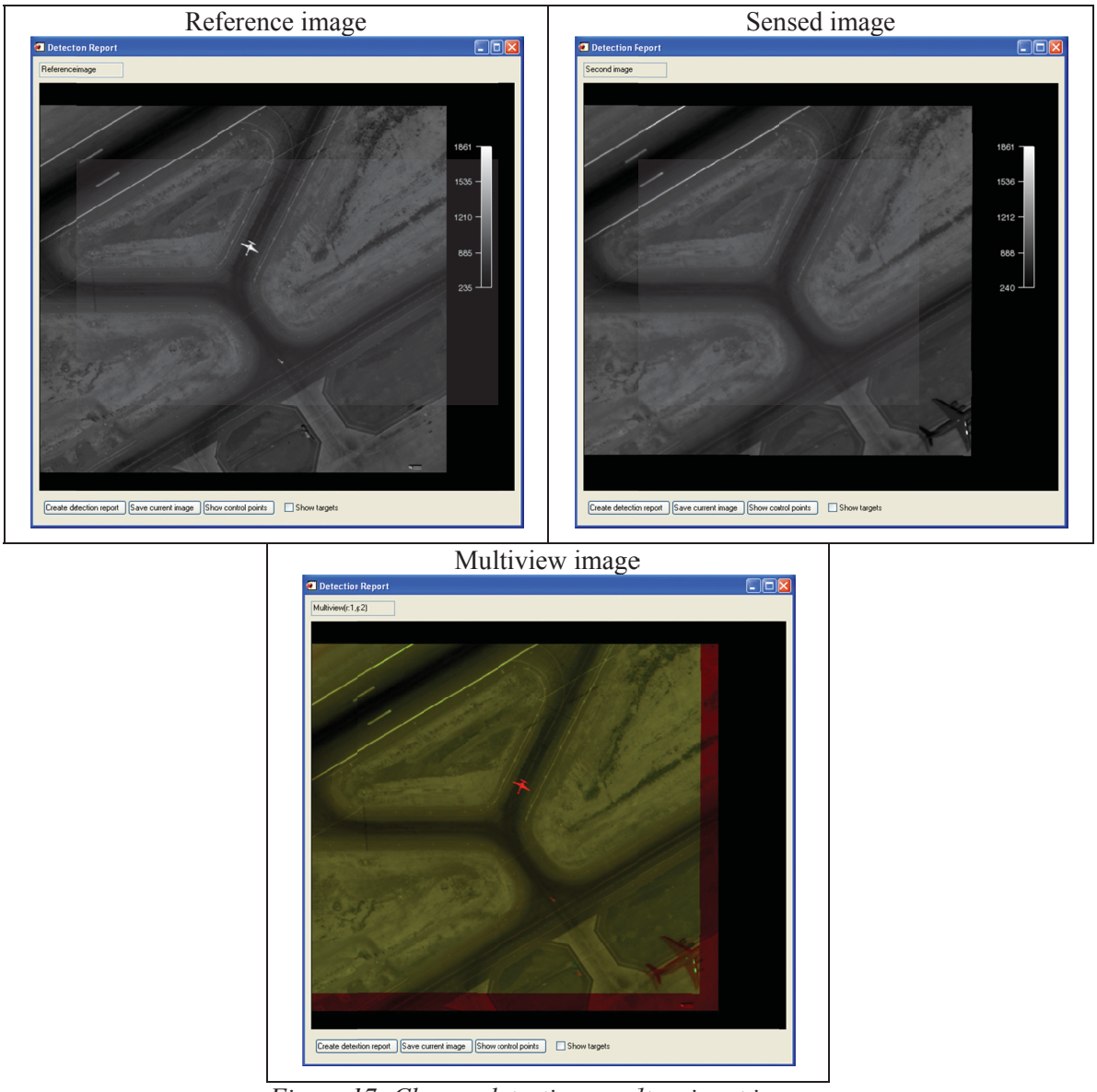

Figure 17: Change detection results – input images

By clicking on the right mouse button, the user can explore change detection results obtained with the implemented algorithms (see figure 18). These images are the result of the change metric calculation, i.e. no threshold has been applied, except for FL Ratio 1, FL Ratio 2 and FL Ratio 3 resulting from the application of different soft thresholds.

The following list details the algorithms used to generate the results shown in figure 18.

1. Advanced difference: simple difference with spatial mitigation of false alarms (as described in section 3.1.2.4);

2. Normalised difference: FL ratio;

3. Advanced normalised difference: FL ratio with spatial mitigation of false alarms;

4. FL ratio 1: FL ratio with spatial mitigation of false alarms, soft threshold set 1;

5. FL ratio 2: FL ratio with spatial mitigation of false alarms, soft threshold set 2; and

6. FL ratio 3: FL ratio with spatial mitigation of false alarms, soft threshold set 3;

The difference between FL1, FL2 and FL3 is the intensity of changes used in the legend. Note that geo-pixel and shading model change metrics are available but are not currently calculated.

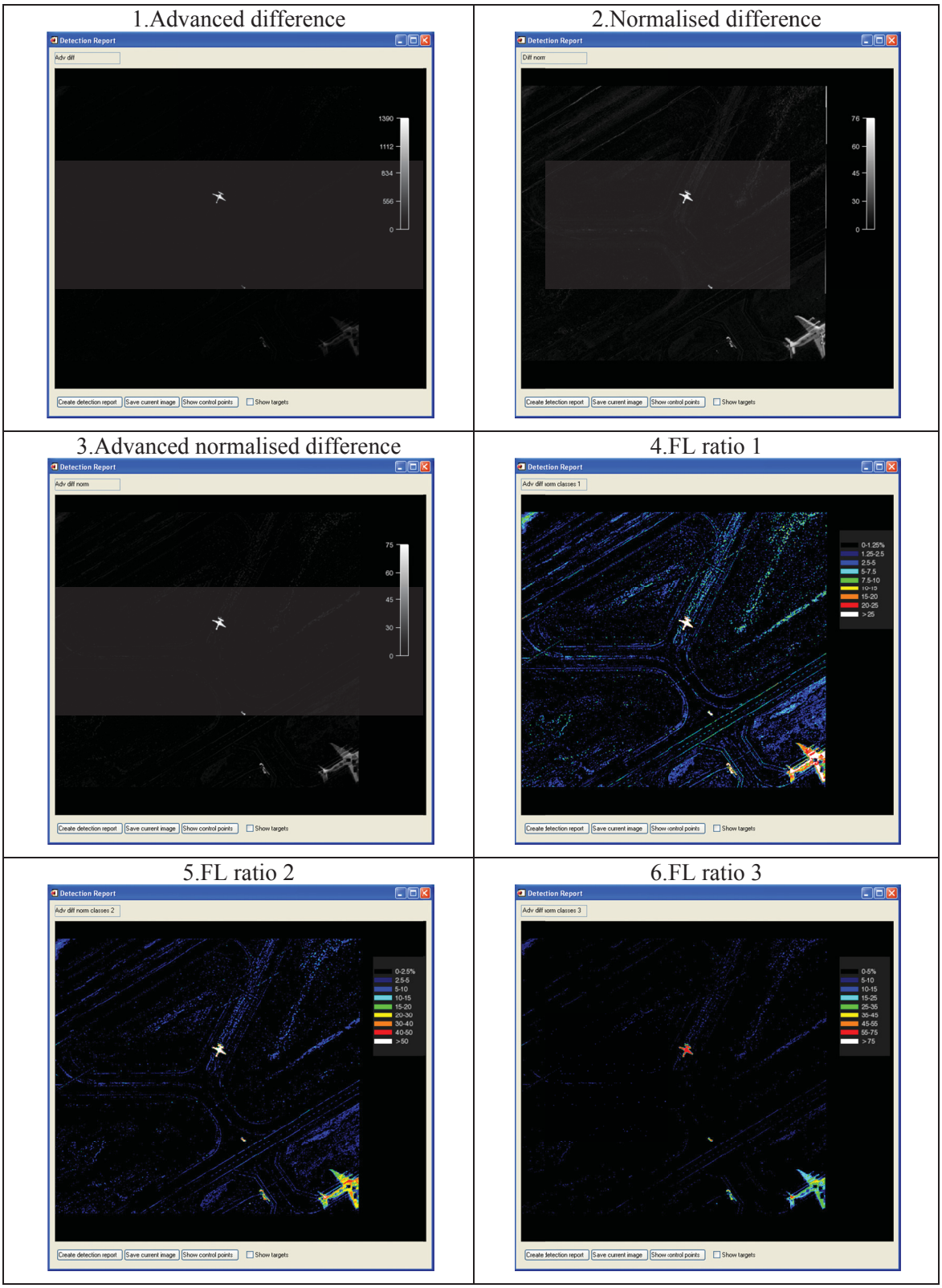

Figure 18: Change detection results – change metrics

The Show targets check box of the interface allows to overlay the currently displayed image with numbered boxes surrounding the detections obtained with the advanced diff change detection algorithm (see Figure 19). The interface is also extended to the right to display a list of detections. The user can then edit this list of detections to confirm or reject a particular detection (see Figure 20), and finally generate a detection report by clicking on the Create detection report button in the lower left corner of the interface.

The Save current image button allows to export the image currently displayed to an image file on disk. The Show control points button opens an interface showing reference image and sensed image side by side, with the control points used to register the two images (see Figure 21).

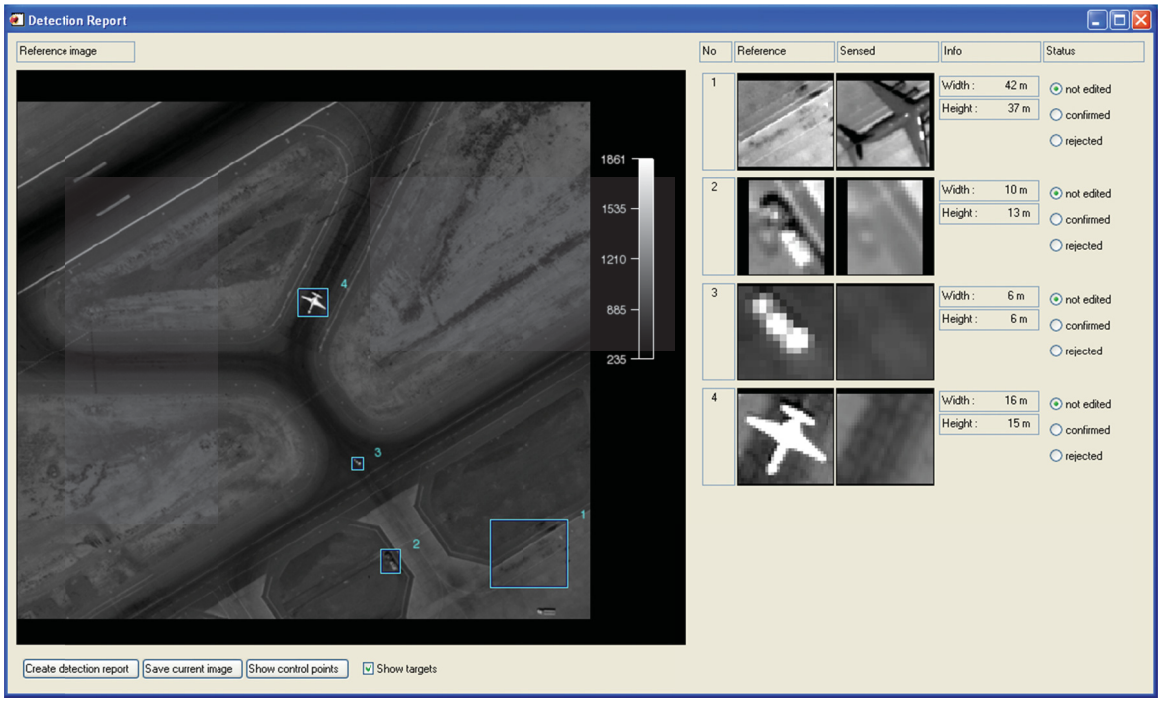

Figure 19: Show targets

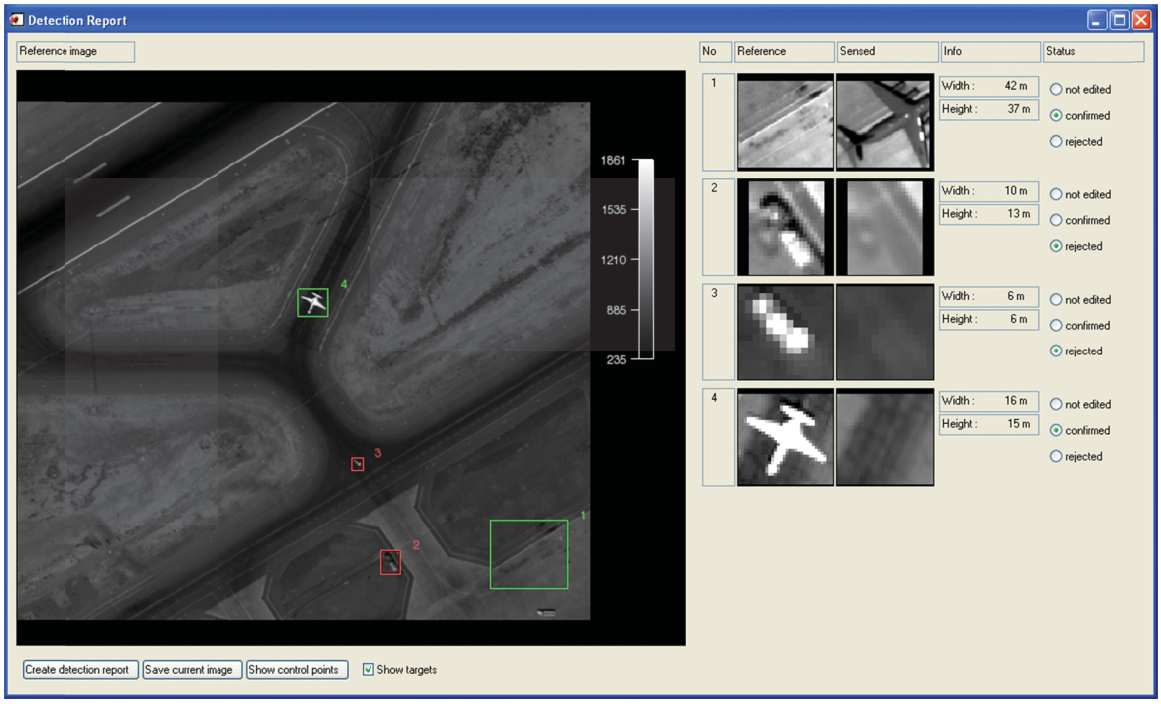

Figure 20: Show targets with edited statuses

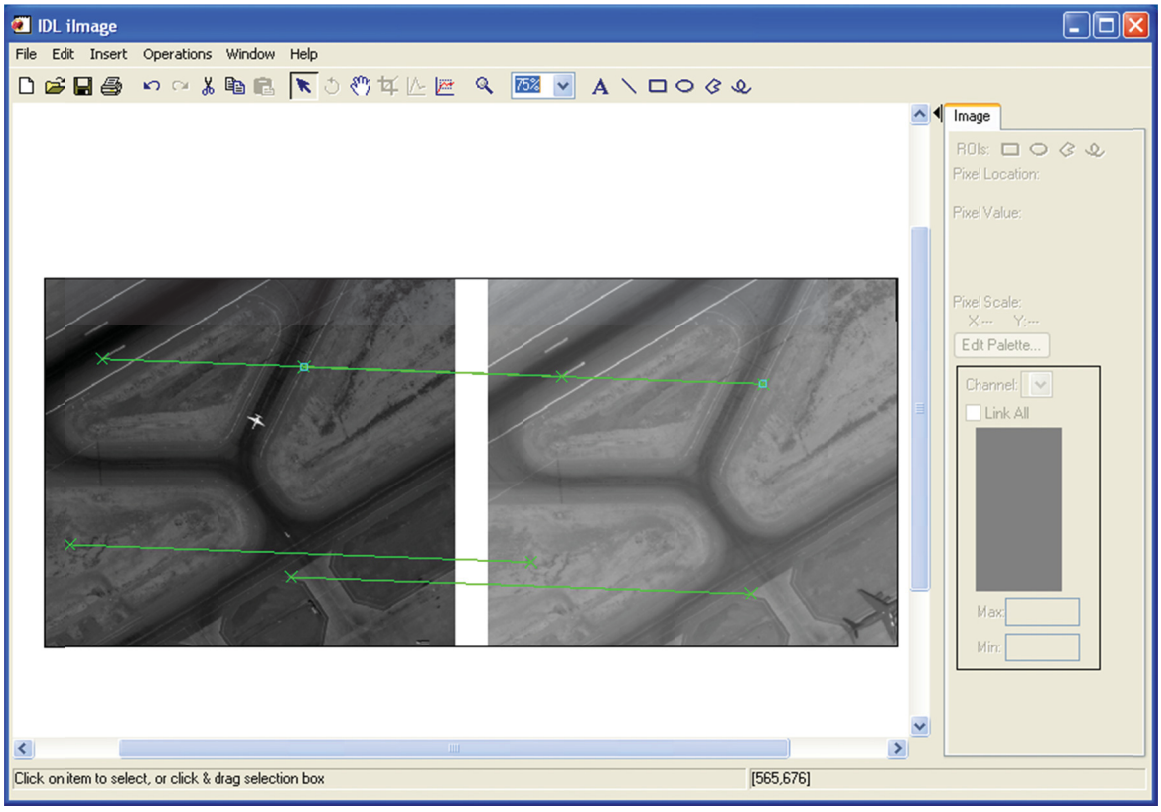

Figure 21: Show control points display

3.2 Batch Vector

Batch vector allows exploring a collection of images in order to find which pair is suitable for change detection on a specific region. The desired region must be specified with a vector file of geographic coordinates. The batch vector tool is ideal to explore a directory of images (library), considering that we have a vector defining a ROI.

3.2.1 Usage

This function takes a vector file (evf extension), as shown in figure 22, and a folder of National Imagery Transmission Format (NITF) images as input (see figure 23). The NITF images can be located in subfolders.

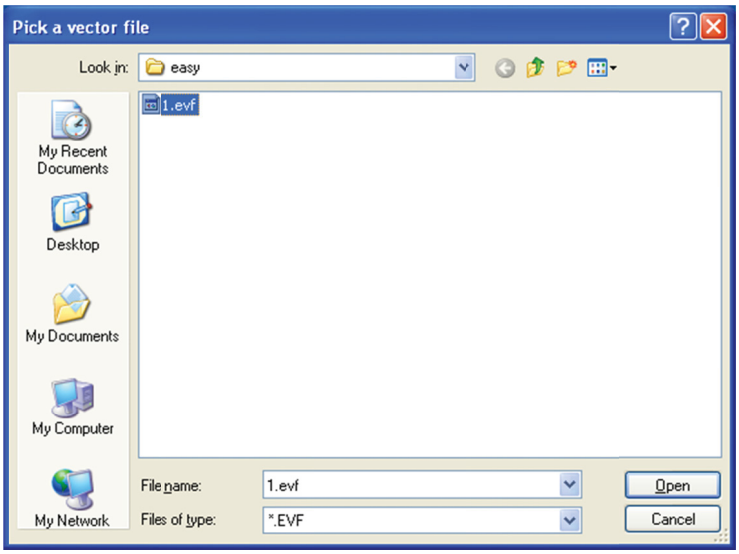

Figure 22: Pick a vector file dialog box

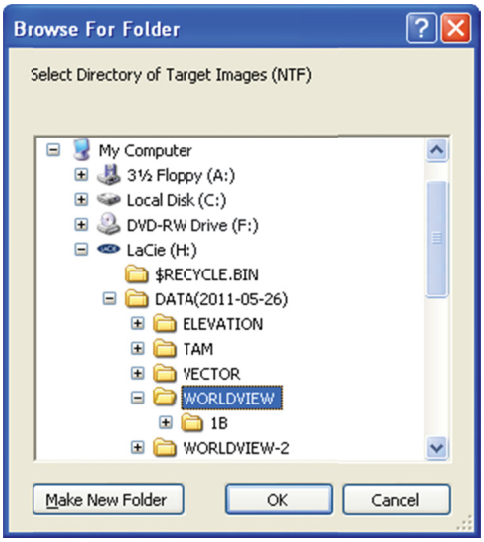

Figure 23: Browse for Folder dialog box

Batch Vector looks for all images in the selected folder and subfolders, and then proceeds to read the metadata from each of the files.

3.2.2 Algorithm

This tool does not implement any particular algorithm. It is more an interface to access the other DTIE algorithms. In fact, in future development of DTIE, the batch vector tool could be the entrance point of DTIE. An outline of the Batch Vector tool algorithm is given in the list below.

1. Find images files (.ntf and .nitf) in selected directory and subdirectories;
2. For each file
    a. Get metadata;
    b. Check if ROI fits in image.

3.2.3 Example result

Figure 24 shows the user interface displayed as a result of the Batch Vector tool operation. The first column lists the filenames of all the NITF files found under the selected folder. The second column indicates whether the region specified by the vector file is included into the image file. The entries in the table are sorted according to this field; first the images where the region of interest was found (ROI fit = 1), then the others (ROI fit = 0). The third column displays the name of the source platform, the fourth and fifth columns indicate the platform attitude, the sixth presents the image ground sampling distance (GSD), the seventh and eighth columns indicate the sun azimuth and elevation at the time of acquisition, and the two last columns list the date and time of acquisition.

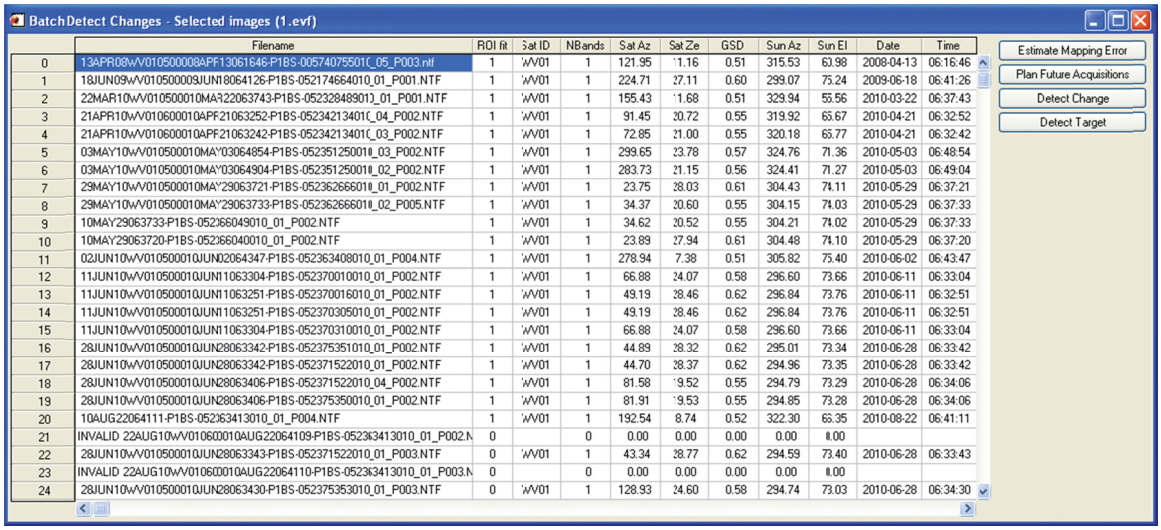

Figure 24: Batch Detect Changes – Selected images dialog box

When the user clicks on an entry in the table, a context menu appears (see Figure 25). The menu allows the user to open the selected image into ENVI, or to copy the filename of the image into the clipboard.

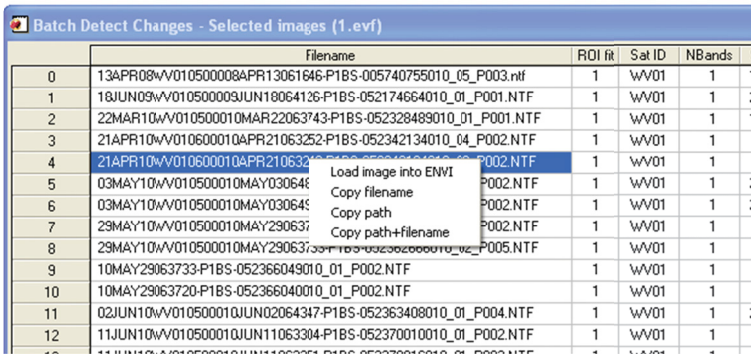

Figure 25: Batch Detect Changes – Context menu

There are four buttons on the right side of the interface. Using these buttons, the user can use the DTIE tools directly from the Batch Vector interface, on the selected image(s).

4 Target detection

The DTIE target detection tool allows detecting a target of interest in an image. This tool can be used alone to detect a given target, but it could also serve as an alternative when change detection is particularly difficult. If the mapping error estimation tool indicates that registration error will be too high to perform change detection with a decent number of false alarms, the target detection tool could be used on the most recent image to report targets of interest since it does not require registration. It could also be used to classify the detected changes found by the change detection algorithm. Changes reported by the change detection tool could be compared to a target database by using comparison metrics provided by the target detection algorithms.

Three target detection algorithms are implemented in DTIE, as shown in Figure 26 below. The next subsections detail each of these algorithms. Test images for target detection are described in Annex A.

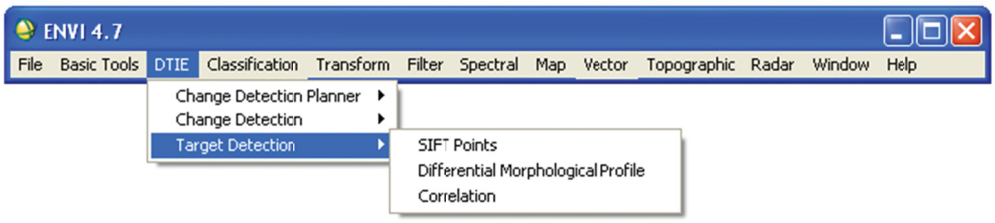

Figure 26: Target Detection ENVI menu

4.1 SIFT Points

SIFT is an interest point detection algorithm developed by Lowe [11]. In his seminal paper, Lowe uses the points found by this algorithm to register two images of the same scene, but also to find targets from a template.

Since the SIFT algorithm provides not only point positions, but also descriptors for each point, it is possible to match the SIFT points found on a target template to the SIFT points found in an image. SIFT also provides orientation and scale estimations, and Lowe proposes to use this information with the Hough transform to select points giving the same estimated pose (orientation and scale). In order to speed up the processing (we expect to work with large satellite images), the Hough transform was replaced by a simple voting algorithm. This is explained in greater detail in subsection 4.1.2.

4.1.1 Usage (SIFT)

The user selects an image (on which he wants to finds targets) and a region of interest, as shown in Figure 27.

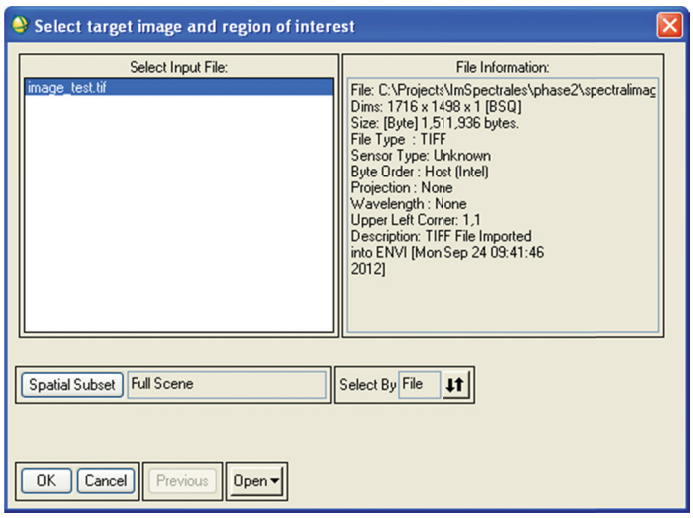

Figure 27: SIFT Target Detection – Select target image and region of interest dialog box

Then, the user selects an object image file to look for, as shown in Figure 28, or press cancel to interactively select the object in the previously specified image (see Figure 29) using the IDL XROI tool.

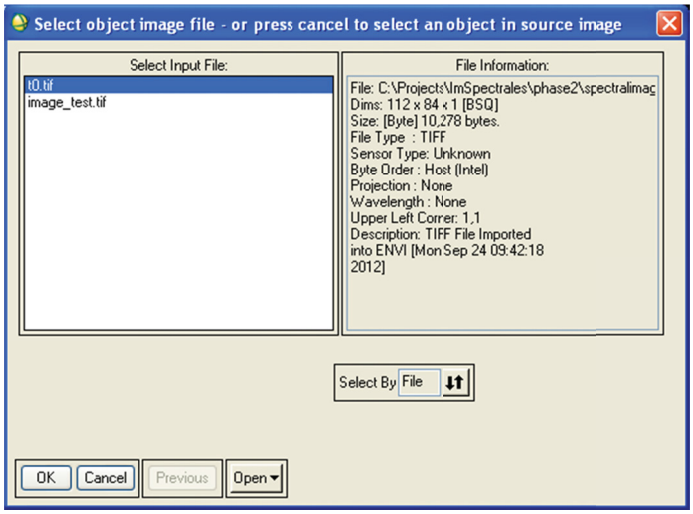

Figure 28: SIFT Target Detection – Select object image file dialog box

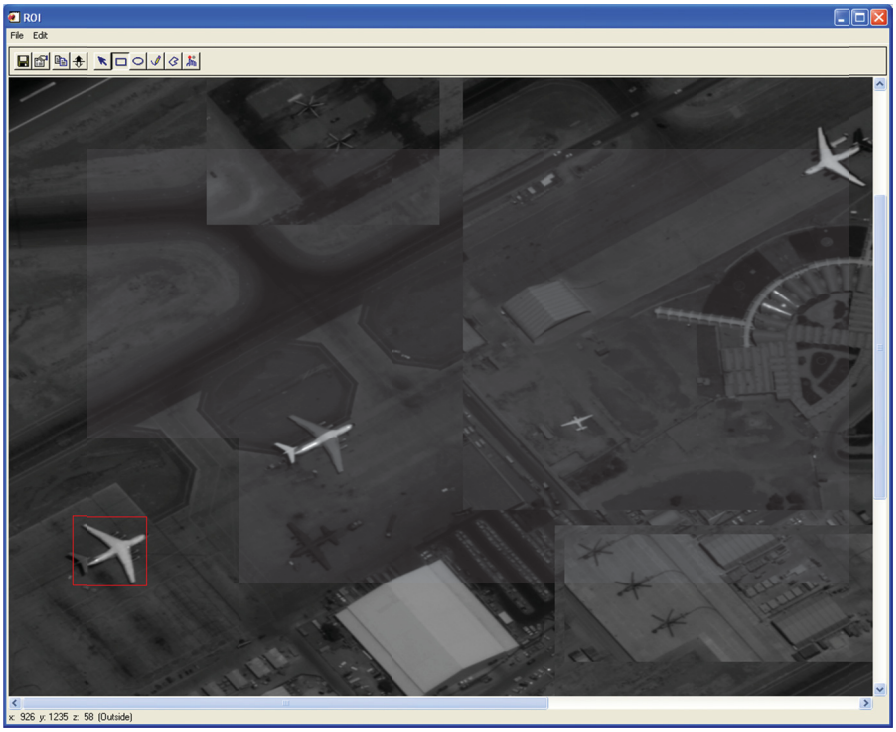

Figure 29: SIFT Target Detection – interactive target selection

After the object image is selected by either method, a progress dialog box is displayed.

4.1.2 Algorithm (SIFT)

As mentioned earlier, this target detection algorithm uses the interest points (and their descriptors) found by SIFT [11]. The steps performed by this algorithm are outlined in the list below.

1. Detect SIFT points on image;
2. Detect SIFT points on object image;
3. Match SIFT points found on both images;
4. Create score image;
5. Apply threshold and report targets.

The first and second steps consist only in applying the SIFT interest points detection algorithm to the selected image and to the object image. In the third step, the points found are matched using their associated descriptors. For each point in one image, its Euclidean distance (in the feature descriptor space) is calculated against all points from the other image. These distances are sorted from smallest to largest. Finally, all points inside a predefined distance ratio are matched to the original point. This is a many-to-many relationship.

The fourth step is where the algorithm diverges from the original target detection algorithm proposed with SIFT. Instead of trying to identify coherent pose estimations, we only consider that

the probability of finding the object in the neighbourhood of a matched interest point increases for each point found. Since SIFT points give an estimated scale and rotation, this information is used to calculate a neighbourhood for each matched point. A score image is thus created by increasing the probability by one in the neighbourhood of each point, and by normalising by the number of points in the object image.

Finally in the last step, the threshold is applied before performing blob detection to identify found targets.

4.1.3 Example result (SIFT)

Figure 30 displays the graphical user interface initially presented to the user for reporting found targets. The selected image is displayed.

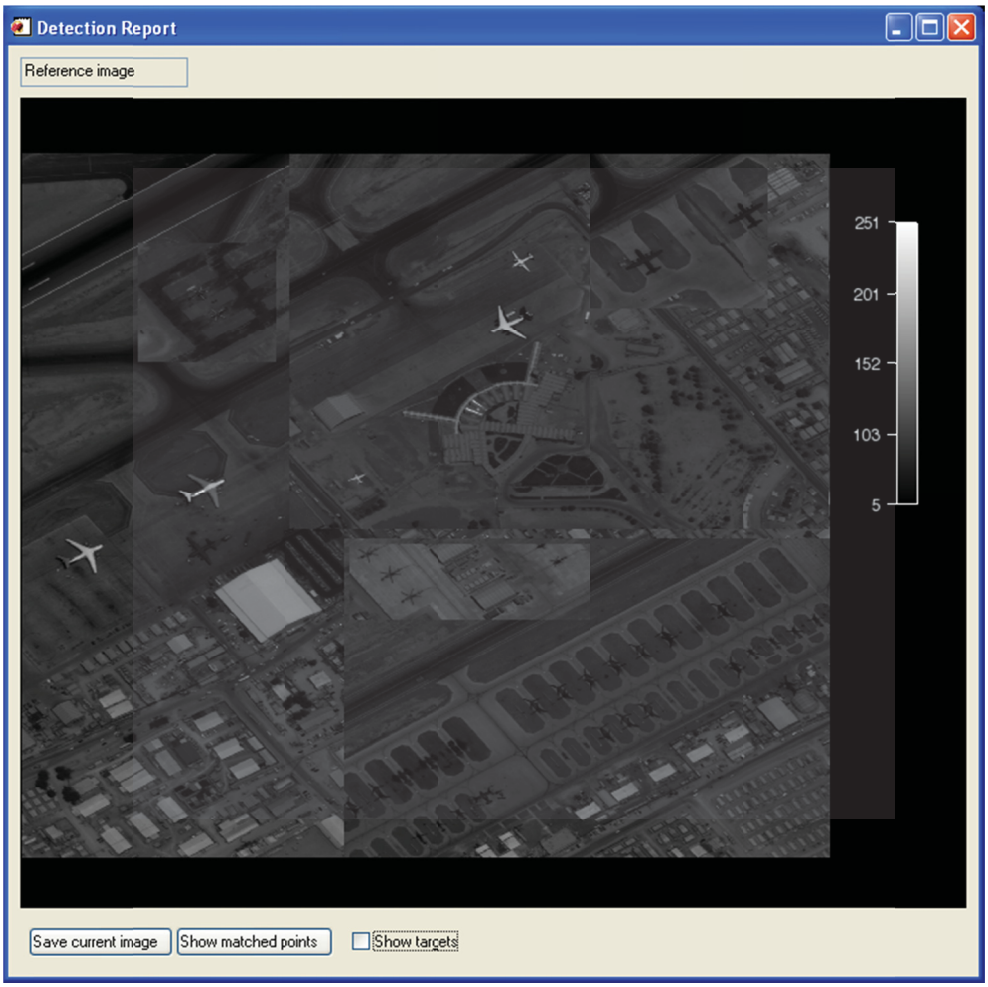

Figure 30: SIFT Detection Report – Reference image dialog box

The Show targets check box overlays the image with indexed boxes on the detected targets, and extends the interface to show detected targets along with the template image (see Figure 31). The

user can also set the status of each detected target to confirmed or rejected and save the image. Clicking on the right button displays the score image instead of the input image (see Figure 32).

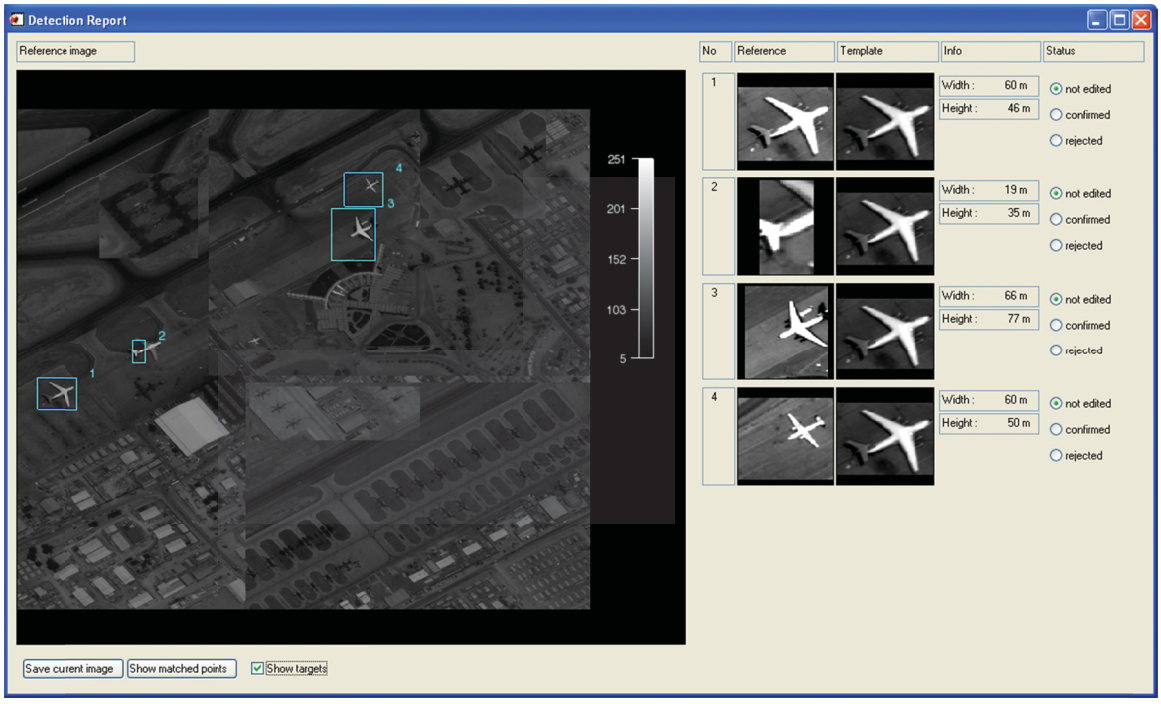

Figure 31: SIFT Detection Report - Reference image with targets

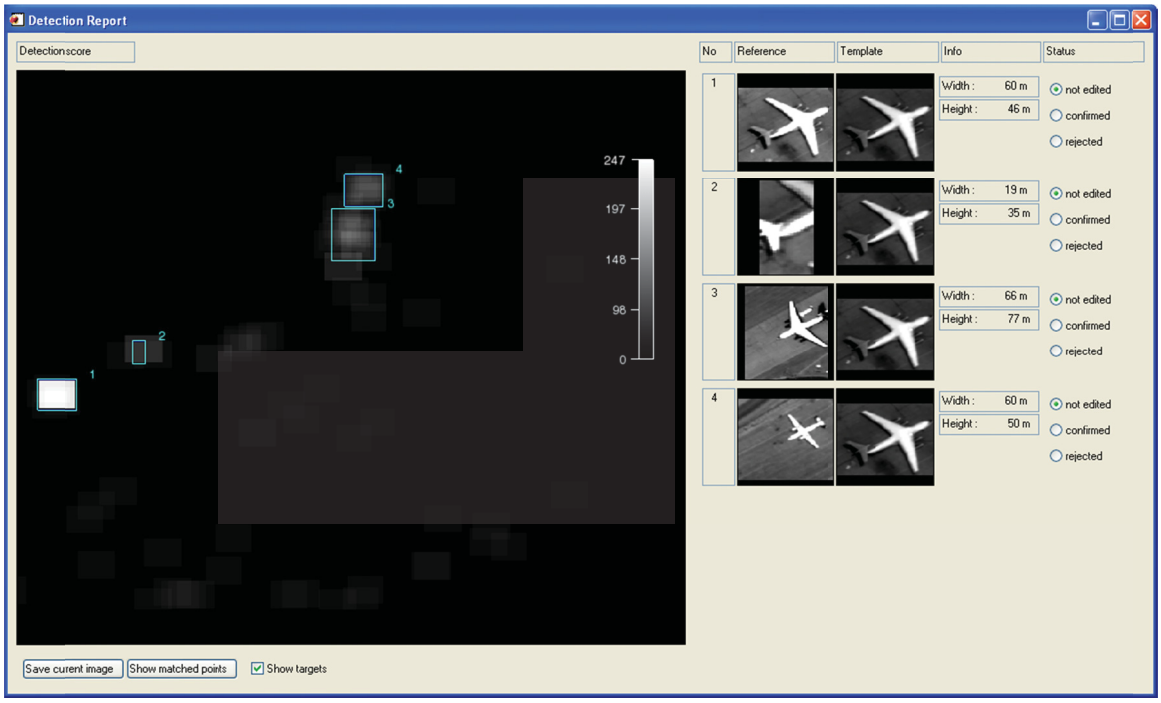

Figure 32: SIFT Detection Report – Detection score with targets

In order to look into detection results, the user is also offered the possibility to see which points were found and matched for a detection, by clicking on the Show matched points button (see Figure 33 and Figure 34).

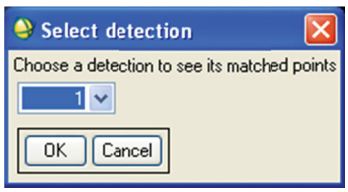

Figure 33: Show matched points – Select detection dialog box

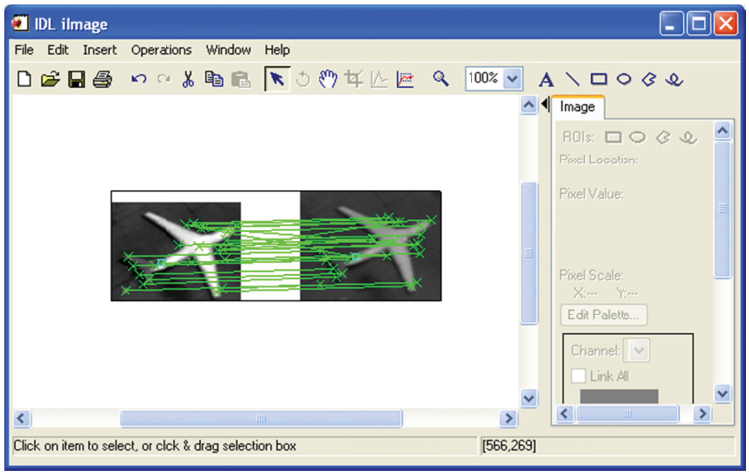

Figure 34: SIFT Target Detection – Show matched points result dialog box

4.2 Differential Morphological Profile

The Differential Morphological Profile (DMP) target detection tool is the application of classical hyperspectral target detection algorithms [20] to differential morphological profiles [19, 21]. Differential morphological profiles, seen as signatures, are fed to the Adaptive Coherence Estimator (ACE) [22] and Constrained Energy Minimization (CEM) [23, 24] algorithms to estimate their similarity against a template signature.

4.2.1 Usage (DMP)

Input image and object selection are done through the same interfaces as SIFT Points target detection (see Figure 27 and Figure 29 in previous section), except that the object image has to be selected interactively, as shown in Figure 35 below.

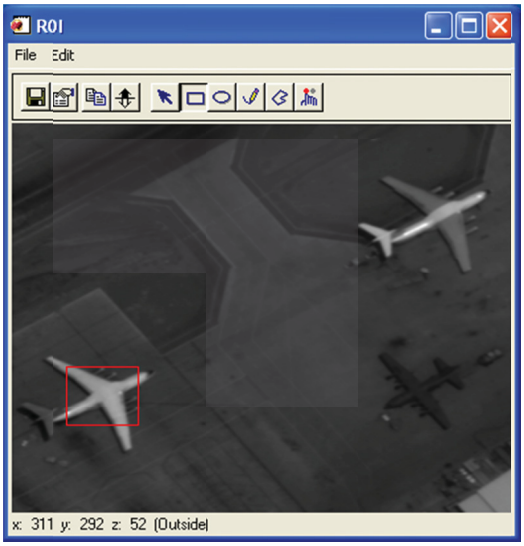

Figure 35: DMP Target Detection – Select template ROI dialog box

Before displaying the detection results, DMP asks the user to select a threshold for results segmentation (see Figure 36). Pixels with values above the threshold will be reported as detections.

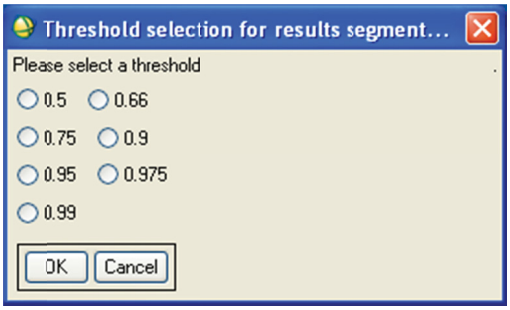

Figure 36: DMP Target Detection – Threshold selection

4.2.2 Algorithm (DMP)

The Differential Morphological Profile target detection algorithm can be separated into the following four steps:

1. Calculate Differential morphological profile

   The Differential Morphological Profile target detection algorithm begins by applying morphological closings and openings of different sizes on the image and on the target to create differential morphological profiles, as described in [21]. The operations made in this step are repeated here to give the user a basic understanding of what the algorithm does.

A morphological profile MP is calculated for each pixel $I(x,y)$ of an image I by applying the opening and closing operators (signalled by o and c subscripts) with size-varying structuring elements s.

The morphological profile at index 0 (both for closing and opening operations) is defined as the original image:

$$MP_o(0) = MP_c(0) = I(x,y) \tag{11}$$

Morphological profiles for indices i from 1 to p are calculated by applying a morphological opening (or closing) with a structuring element s of size i:

$$MP_o(i) = O_{si}\big(I(x,y)\big) \qquad for\ i = 1, \dots, p \tag{12}$$

$$MP_c(i) = C_{si}(I(x,y)) \qquad for\ i = 1, \dots, p \tag{13}$$

The Differential Morphological Profile DMP is calculated by subtracting the morphological layers from two consecutive structuring element sizes.

$$DMP_o(i) = MP_o(i-1) - MP_o(i) \qquad for\ i = 1, \dots, p \tag{14}$$

$$DMP_c(i) = MP_c(i-1) - MP_c(i) \qquad for\ i = 1, \dots, p \tag{15}$$

The closing and opening differential profiles are then concatenated to obtain a full profile

$$DMP(i) = \begin{cases} DMP_o(i) & for\ i = 1, \dots, p \\ DMP_c(-i) & for\ i = -1, \dots, -p \end{cases} \tag{16}$$

Finally, each pixel differential profile is normalised

$$nDMP(i) = \frac{DMP(i)}{\sum_{j=-p}^{p} DMP(j)} \qquad for\ i = -p, \dots, p \tag{17}$$

2. Calculate target signature

The template signature is obtained by taking the nine normalised differential profiles in the template neighbourhood. Using these nine profiles, six signatures are generated:

i. Min: the minimum values of the nine normalised differential profiles of the neighbourhood;
ii. Max: the maximum values;
iii. Avg: the average values;

iv. Center: the values at the center of the neighbourhood, i.e. the original template position;
v. Avg+Std: the average values plus the standard deviations; and
vi. Avg-Std: the average values minus the standard deviations.

This set of signatures for the template adds robustness to the target detection algorithm by characterising the target and its neighbourhood. The idea behind this approach is that a target is not characterised by a unique signature.

3. Hyperspectral target detection

A differential morphological profile can be interpreted as spectral data. Instead of having a value for a series of wavelengths, we have a value for a series of structuring element sizes. The structuring element size is linked to a scale in a similar way as the wavelength. Therefore, hyperspectral detection algorithms [20] can be used here to evaluate similarity of a profile against the template profile.

The Adaptive Coherence Estimator (ACE) [22] and Constrained Energy Minimization (CEM) [23, 24] are used to estimate the distance between two spectra. The reader is referred to the cited papers for further information on those algorithms.

ACE and CEM are both applied on all six signatures generated in step 2. Afterwards, the maxima of all ACE results are combined with the maxima of all CEM results by taking the minimum of both results. This way, the best ACE result is compared to the best CEM result, and the minimum of these results is the final result.

4. Threshold

A threshold is applied on the score image resulting from the hyperspectral target detection. The user is presented with a choice of 0.5, 0.66, 0.75, 0.90, 0.95, 0.975, 0.99 for threshold. A higher threshold results in fewer false alarms, but has a smaller probability of finding good targets.

4.2.3 Example result (DMP)

Figure 37 shows the dialog box presented to the user as a result of target detection. The user can check the Show targets check box to display detected targets as overlaid boxes on the input image, along with the list of detection on the right (see Figure 38). The user can confirm or reject the detections. The user can also display the detection score by clicking the right button of the mouse (see Figure 39).

Figure 37: DMP Target Detection – Reference image dialog box

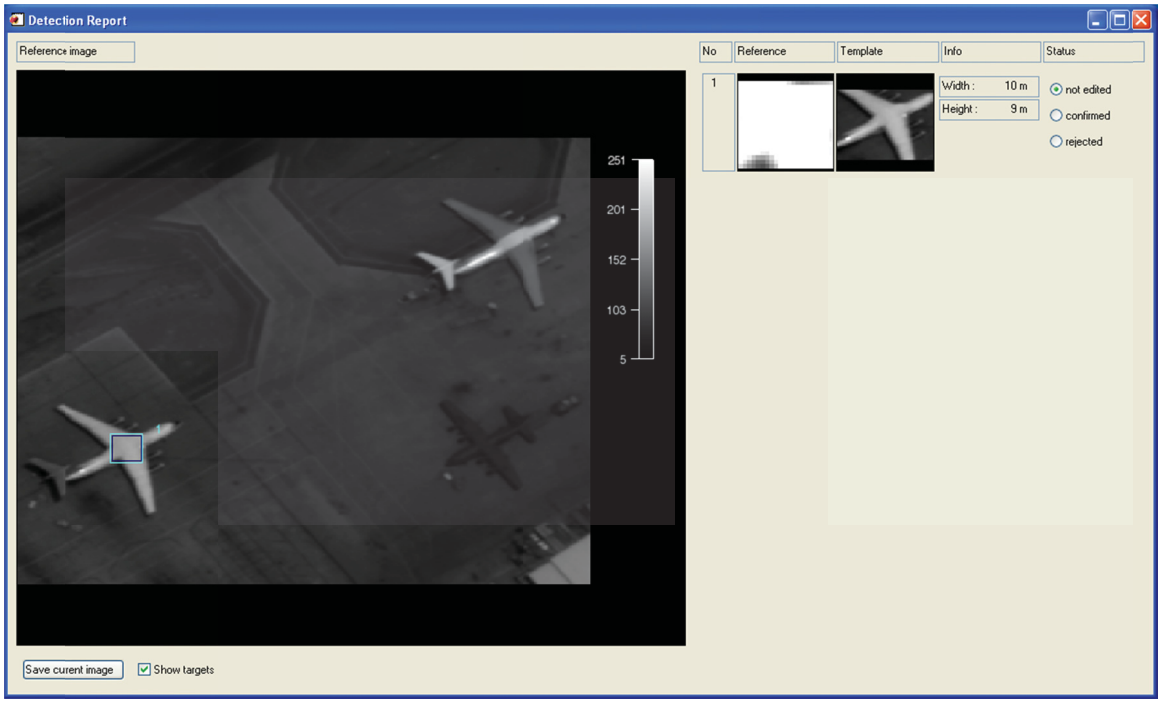

Figure 38: DMP Target Detection – Show targets dialog box

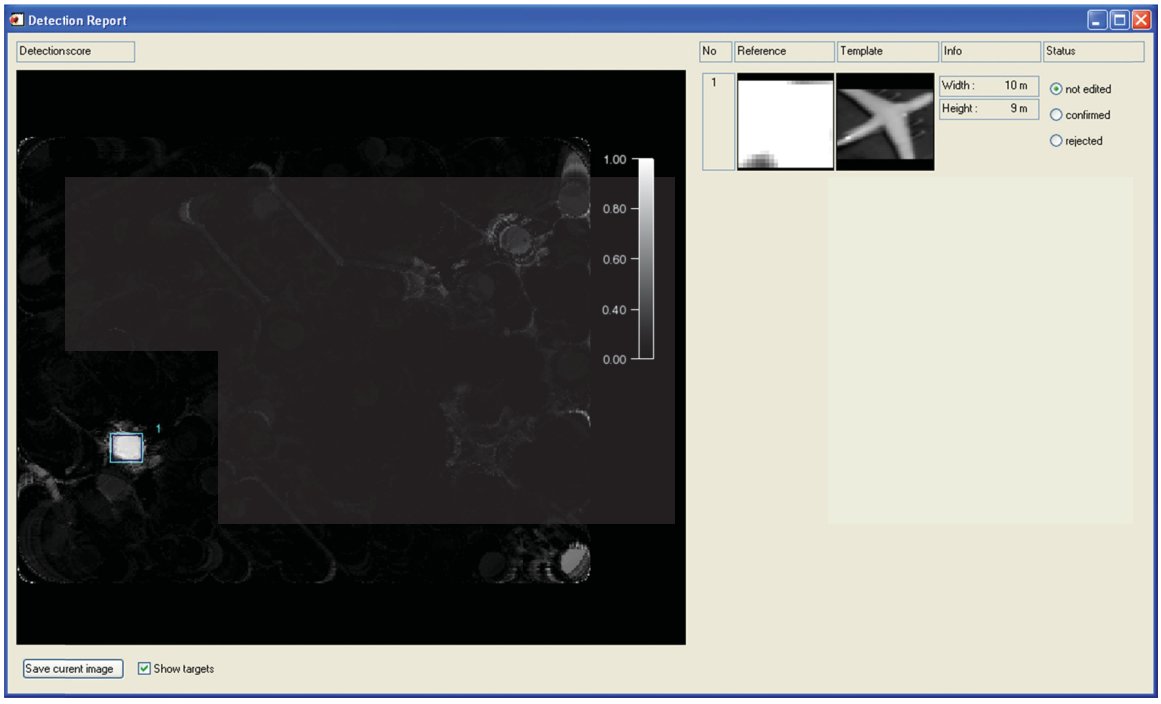

Figure 39: DMP Target Detection – Detection score dialog box

4.3 Correlation

A classical normalised correlation target detection algorithm has been implemented in DTIE to serve as a baseline for evaluating other algorithms performance. This algorithm yields intuitive and predictable results but at the cost of a very high computation time. The implementation presented is optimised, but still offer very slow speed. However, this algorithm is ideal for parallel processing and deserves to be evaluated.

4.3.1 Usage (correlation)

The input image and target object are selected by the user in the same way as with the SIFT Points algorithm (see Figure 27, Figure 28 and Figure 29). When the target detection process is launched, a progress window appears to inform the user of the process.

4.3.2 Algorithm (correlation)

The first step is to extract the correlation template. The diagonals from the object image are extracted in order to get a 45-degree rotation invariant representation (as shown in Figure 40). This speeds up normalised correlation calculation.

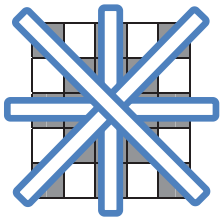

Figure 40: Correlation template

For each location in the input image, the correlation template is extracted and compared to the object template by calculating the normalised correlation between the two templates.

Normalised correlation is of common usage in pattern recognition, and is given by

$$c = \frac{N(\sum IO) - (\sum I)\sum O}{\sqrt{\left[[N\sum I^2 - (\sum I)^2][N\sum O^2 - (\sum O)^2]\right]}} \tag{18}$$

where N is the number of pixels in the object, I is the image part to compare, O the object and $\sum$ is the usual summation operation. The normalisation accounts for uniform changes in intensity.

The actual version of correlation available in DTIE is not invariant to rotation and scale. However, the implementation using diagonals extraction allows easily extending the algorithm for some rotation and scaling invariance. It was not implemented because that would cause the algorithm to be even slower.

4.3.3 Example result (correlation)

Figure 41 shows the result of applying the correlation target detection algorithm to the same example as before. Figure 42 shows the score image for the same example.

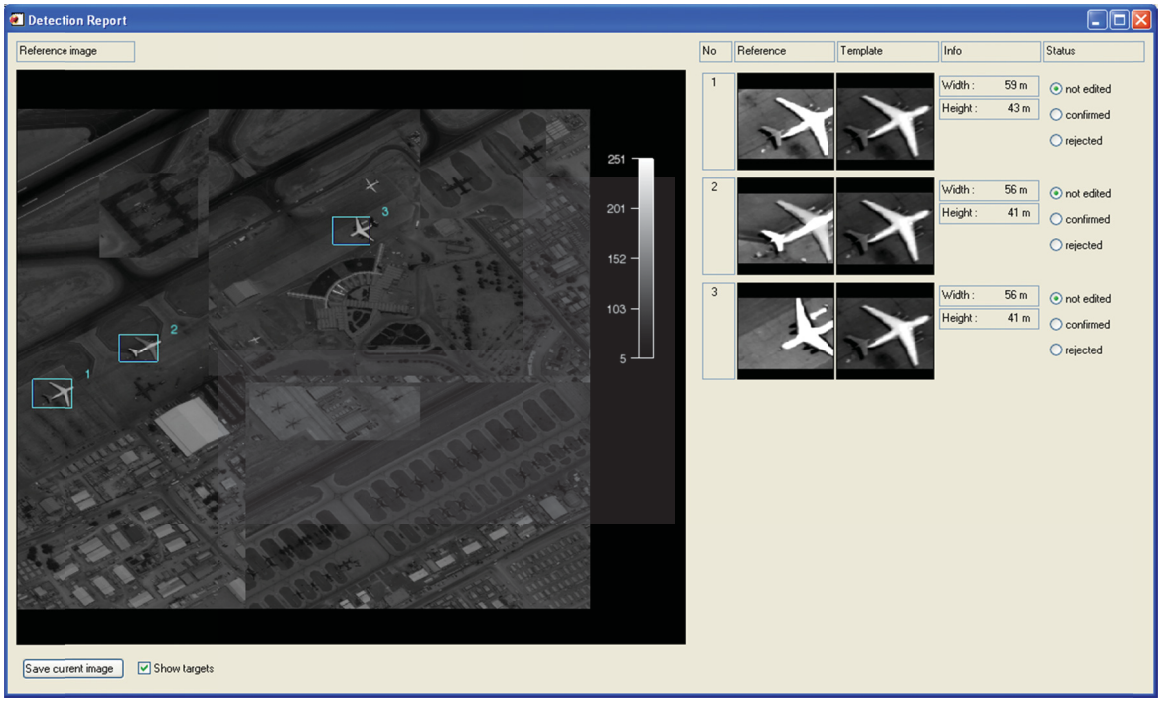

Figure 41: Detection Report - Correlation

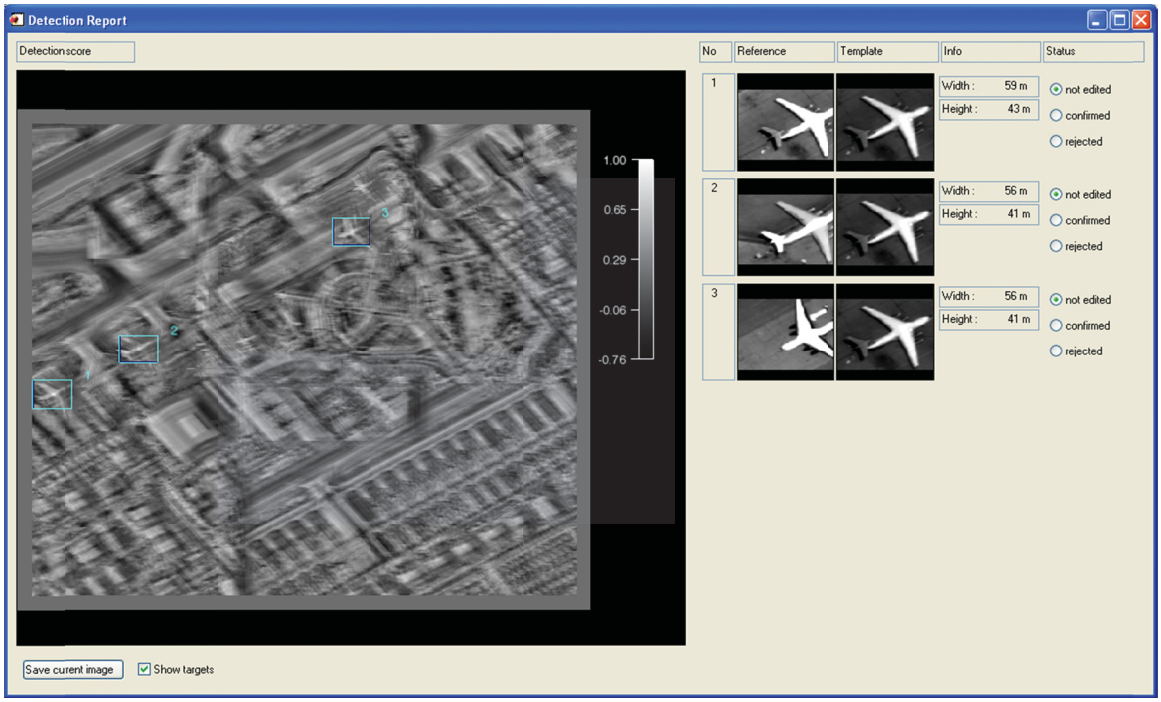

Figure 42: Detection Report – Correlation score image

4.4 Comparison

DTIE proposes three target detection tools to the user. These tools have different strengths and weaknesses. The salient points are summarised in Table 2.

Table 2: Target detection algorithms comparison

Algorithm	Invariance	Speed	Notes
SIFT-based	Rotation, Scale, some illumination	Fast	
Differential Morphological Profile	Rotation	Intermediate	Could be parallelised for faster execution.
Normalised Correlation	Illumination	Very slow	Could be parallelised for faster execution. Could be extended to provide some invariance to rotation and scale, but at the price of speed.

5 Conclusion

Military surveillance using remotely sensed data requires a lot of work from image analysts. The quantity of imagery available being larger than processing capability, many images are left unused. These images could contain data of interest. A tool, which would exploit these images, even only a fraction of them, would be a valuable asset.

Automatic processing of images for change detection would be ideal. However, it is not yet possible to get a high probability of detection with a sufficiently low false alarm rate. By predicting which pair of images would lead to small registration errors and low false alarm rate, it becomes possible to perform automatic or assisted processing of otherwise unused images.

The goal of this project was to select suitable pairs of images for automatic or assisted processing. A suite of tools for imagery exploitation was developed to help an image analyst in selecting the best candidate pairs for automatic processing. The results are editable by the analyst in order to ease verification and report generation.

The first part of this project [1] aimed at predicting registration error. This error must be the lowest possible to reduce the false alarm rate in change detection. The second part of the project, presented in this report, aimed at integrating the registration error prediction tool previously developed into a suite of tools available in Exelis ENVI/IDL. This suite of tools demonstrates the different steps that could lead to automatic processing of a selected subset of images.

The first tools, “Estimate Mapping Error” and “Plan Future Acquisitions”, allow finding suitable regions for change detection, and planning acquisitions meeting the requirements for easy change detection, respectively. The second set of tools, “Change Detection” and “Batch Processing”, implements classical change detection algorithms, and allows the user to select a suitable pair of images from an image directory. The third and last set of tools contained under “Target Detection”, proposes three target detection algorithms to find a known target in an image.

All these tools embody a particular aspect, or step, of automated image processing for change detection. The suite can be used to evaluate, demonstrate or enhance each of these aspects before integrating them into a unique tool. The tools can also be useful to image analysts to support part of their work, and to evaluate their needs for such tools.

6 Future work

The suite of imagery exploitation tools could be deployed to image analysts for evaluation, and to identify if one of them could be used alone with minor modifications.

The performance of all the tools presented here could be enhanced. Especially change detection, which only proposes classical change detection algorithms. A function predicting radiometric normalisation performance could also be added. This would be of interest but many challenges remains before reaching an acceptable solution. Among them, the unavailability of precise digital elevation data and the lack of information about the materials being observed. This impedes using bidirectional reflectance distribution function BRDF models to predict image radiometric content.

Finally, this suite of tools could be integrated into a single tool performing change detection on a subset of suitable pair of images. The user would have to select a source image and a geographic region of interest. The tool would automatically find suitable images, perform change detection, and present a report to an image analyst for revision. This revision could be used to fill a database of known false alarms to stop reporting them in the future, and a database of good detections that could be used for target detection when change detection is deemed too difficult or impractical.

References

[1] V. Labbé, "Prediction of Image Registration Performance" , *AEREX Report No. 2011-92854-2,* 2012.

[2] R. Radke*, et al.*, "Image change detection algorithms: a systematic survey" , *Image Processing, IEEE Transactions on,* vol. 14, pp. 294-307, 2005.

[3] L. Brown, "A survey of image registration techniques" , *ACM computing surveys (CSUR),* vol. 24, pp. 325-376, 1992.

[4] B. Zitova and J. Flusser, "Image registration methods: a survey" *, Image and vision computing,* vol. 21, pp. 977-1000, 2003.

[5] M. Wyawahare*, et al.*, "Image Registration Techniques: An overview" , *International Journal of Signal Processing, Image Processing and Pattern Recognition,* vol. 2, pp. 1-5, 2009.

[6] J. Li and N. Allinson, "A comprehensive review of current local features for computer vision" , *Neurocomputing,* vol. 71, pp. 1771-1787, 2008.

[7] T. Tuytelaars and K. Mikolajczyk, "Local invariant feature detectors: A survey" , *Foundations and Trends® in Computer Graphics and Vision,* vol. 3, pp. 177-280, 2008.

[8] A. Montero*, et al.*, "Robust Detection of Corners and Corner-line links in images" , 2010.

[9] C. Harris and M. Stephens, "A combined corner and edge detector" , 1988, p. 50.

[10] J. Noble, "Finding corners" , *Image and vision computing,* vol. 6, pp. 121-128, 1988.

[11] D. Lowe, "Distinctive image features from scale-invariant keypoints" , *International Journal of Computer Vision,* vol. 60, pp. 91-110, 2004.

[12] T. Lindeberg, "Feature detection with automatic scale selection" , *International Journal of Computer Vision,* vol. 30, pp. 79-116, 1998.

[13] K. Mikolajczyk and C. Schmid, "Scale & affine invariant interest point detectors" , *International Journal of Computer Vision,* vol. 60, pp. 63-86, 2004.

[14] E. Rosten and T. Drummond, "Fusing points and lines for high performance tracking" , 2005, pp. 1508-1515.

[15] M. A. Fischler and R. C. Bolles, "Random sample consensus: a paradigm for model fitting with applications to image analysis and automated cartography" , *Communications of the ACM,* vol. 24, pp. 381-395, 1981.

[16] R. Schowengerdt, *Remote sensing: models and methods for image processing*: Academic Pr, 2007.

[17] K. Skifstad and R. Jain, "Illumination independent change detection for real world image sequences* 1" , *Computer Vision, Graphics, and Image Processing,* vol. 46, pp. 387-399, 1989.

[18] A. Elgammal*, et al.*, "Non-parametric model for background subtraction" , *Computer Vision—ECCV 2000,* pp. 751-767, 2000.

[19] F. Leduc*, et al.*, "A suite of tools for imagery analysis and change detection" , presented at the SAEF/EOPAB conference, Chantilly, VA, 2011, DRDC Valcartier SL2012-147.

[20] D. Manolakis*, et al.*, "Hyperspectral image processing for automatic target detection applications" , *Lincoln Laboratory Journal,* vol. 14, pp. 79-116, 2003.

[21] J. Chanussot*, et al.*, "Classification of remote sensing images from urban areas using a fuzzy possibilistic model" , *Geoscience and Remote Sensing Letters, IEEE,* vol. 3, pp. 40-44, 2006.

[22] S. Bidon, *et al.*, "The adaptive coherence estimator is the generalized likelihood ratio test for a class of heterogeneous environments" , *Signal Processing Letters, IEEE,* vol. 15, pp. 281-284, 2008.

[23] C. I. Chang, *et al.*, "Generalized constrained energy minimization approach to subpixel target detection for multispectral imagery" , *Optical Engineering,* vol. 39, pp. 1275-1281, 2000.

[24] Q. Du, *et al.*, "A comparative study for orthogonal subspace projection and constrained energy minimization" , *Geoscience and Remote Sensing, IEEE Transactions on,* vol. 41, pp. 1525-1529, 2003.

This page intentionally left blank.

Annex A Images Dataset

DTIE tools were tested on an example dataset. This dataset consists of satellite images and digital elevation data. This section presents the characteristics of the test dataset.

A.1 Images

A.1.1 Change detection

Change detection tools were tested using a set of DigitalGlobe Worldview-1 and Worldview-2 satellite images. These images are in the NITF format and contain acquisition metadata. The image dataset has accompanying shapefiles giving the geographic position of the images. Figure shows positions of WorldView-1 panchromatic images around the KAF airport in Esri ArcGIS Explorer.

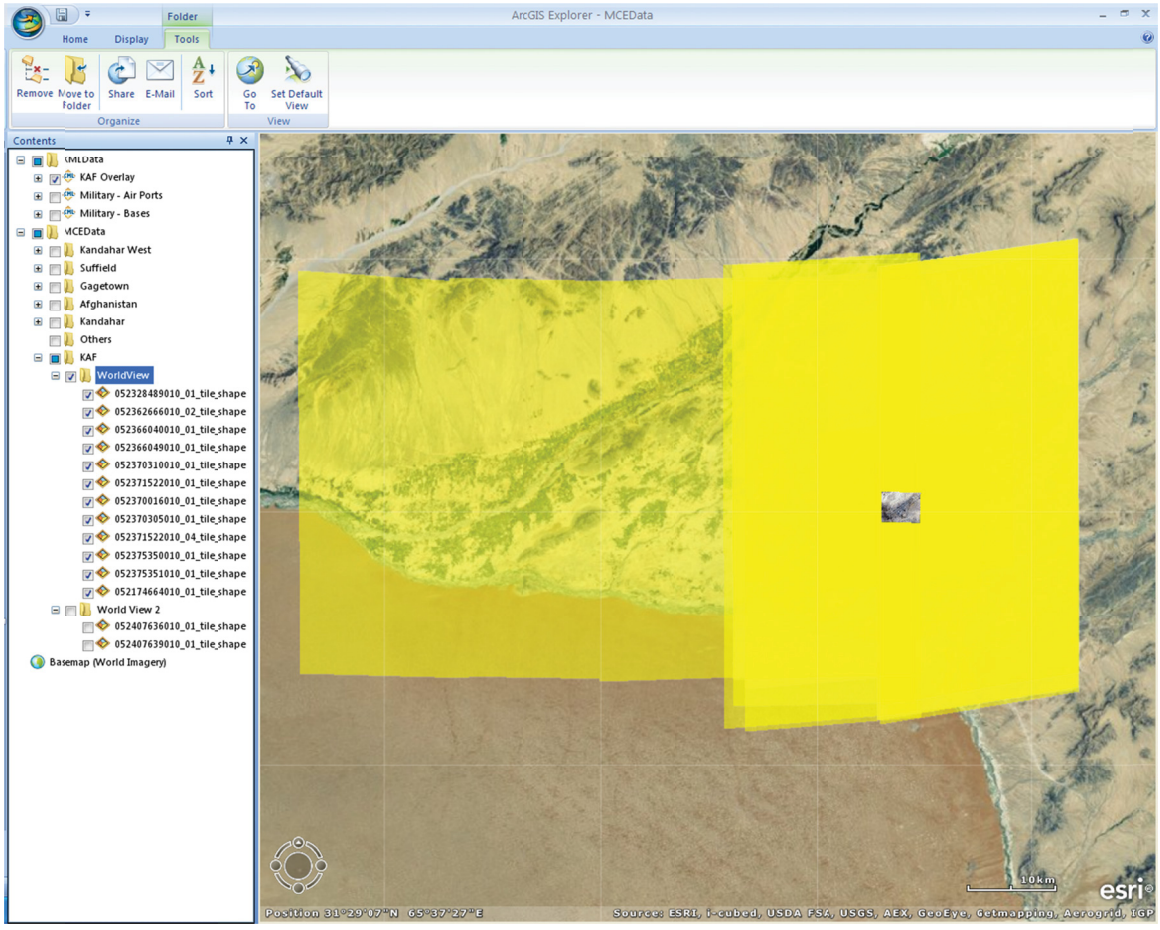

Figure A-1: Dataset geographic position in Esri ArcGIS Explorer

WorldView-1 acquires panchromatic images (400-900 nm) with a Ground Sample Distance (GSD) of about 50 cm.

WorldView-2 provides panchromatic images (450-800 nm) at 46 cm GSD and multispectral images (4 colors: blue, green, red, near-IR) at 1.85 m GSD.

A.1.2 Target detection

It is convenient to test target detection algorithms on an image containing many targets, and on structures similar to targets likely to generate false alarms. Figure A-2, an assembly of many images, shows many targets of different sizes and contrasts. It was used to test the DTIE target detection algorithms. It is a 1716 x 1498 pixels, 8-bit gray-scale image.

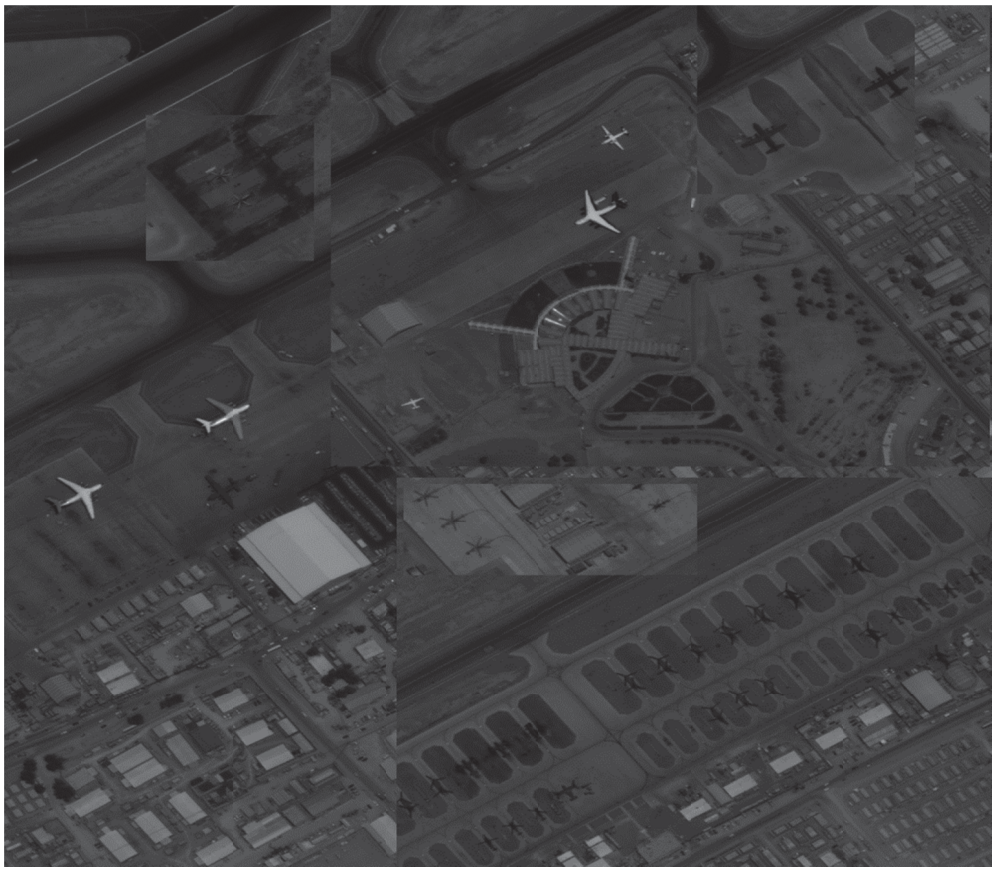

Figure A-2: Target detection test image

A.2 Digital elevation data

The digital elevation data used for the examples in this report is a collection of SRT2 directories. The DTED have a resolution of about 26 meters. Annex B lists the directories and the geographic limits of the region covered.

To speed up access to DTED data, the available DTED are preprocessed by calling the procedure `createdtedindex, dir, dtedindex`. This procedure looks for all "dted" in the specified directory and creates an index, a list of structures, in which each element contains

- Filename
- Minimum latitude
- Maximum latitude
- Minimum longitude
- Maximum longitude
- Directory

Annex B DTED Dataset

As a reference for future use of this DTED dataset, Table lists, for each directory of DTEDs, the minimum and maximum latitude and longitude of all the DTEDs in the specified directory.

Table B-1: SRT2 DTED geographic limits

Directory	lat_min	lat_max	lon_min	lon_max
SRT201_2	52	60	-177	-106
SRT202_2	52	60	-106	-43
SRT203_2	52	60	-14	40
SRT204_2	52	60	40	82
SRT205_2	52	60	82	120
SRT206_2	52	60	120	180
SRT207_2	42	52	-180	-110
SRT208_2	42	52	-110	-92
SRT209_2	42	52	-92	-74
SRT210_2	42	52	-74	-52
SRT211_2	42	52	-11	12
SRT212_2	42	52	12	30
SRT213_2	42	52	30	48
SRT214_2	42	52	48	66
SRT215_2	42	52	66	82
SRT216_2	42	52	82	100
SRT217_2	42	52	100	118
SRT218_2	42	52	118	136
SRT219_2	42	52	136	180
SRT220_2	30	42	-125	-114
SRT221_2	30	42	-114	-100
SRT222_2	30	42	-100	-86
SRT223_2	30	42	-86	-31
SRT224_2	30	42	-29	0
SRT225_2	30	42	0	16
SRT226_2	30	42	16	30
SRT227_2	30	42	30	44
SRT228_2	30	42	44	58
SRT229_2	30	42	58	70
SRT230_2	30	42	70	82
SRT231_2	30	42	82	96
SRT232_2	30	42	96	110
SRT233_2	30	42	110	124

Directory	lat_min	lat_max	lon_min	lon_max
SRT234_2	30	42	124	144
SRT235_2	16	30	-179	-102
SRT236_2	14	30	-102	-86
SRT237F_2	17	21	-75	-68
SRT237_2	14	30	-86	-60
SRT238_2	14	30	-26	-10
SRT239_2	14	30	-10	0
SRT240_2	14	30	0	10
SRT241_2	14	30	10	20
SRT242_2	14	30	20	30
SRT243_2	14	30	30	40
SRT244_2	14	30	40	50
SRT245_2	14	30	50	60
SRT246_2	15	30	60	74
SRT247_2	14	30	74	82
SRT248_2	16	30	82	92
SRT249_2	14	30	92	102
SRT250_2	14	30	102	110
SRT251_2	15	30	110	120
SRT252_2	14	30	120	170
SRT253_2	0	14	-177	-72
SRT254_2	0	14	-72	-60
SRT255_2	0	14	-60	-49
SRT256_2	4	14	-17	-6
SRT257_2	4	14	-6	6
SRT258_2	0	14	6	18
SRT259_2	0	14	18	30
SRT260_2	0	14	30	42
SRT261_2	0	14	42	55
SRT262_2	0	14	72	82
SRT263_2	0	14	92	100
SRT264_2	0	14	100	114
SRT265_2	0	14	114	128
SRT266_2	0	14	128	174
SRT267_2	-12	0	-175	-72
SRT268_2	-12	0	-72	-60
SRT269_2	-12	0	-60	-48
SRT270_2	-12	0	-48	-32
SRT271_2	-12	0	-15	20

Directory	lat_min	lat_max	lon_min	lon_max
SRT272_2	-12	0	20	32
SRT273_2	-12	0	32	74
SRT274_2	-12	0	96	112
SRT275_2	-12	0	112	124
SRT276_2	-12	0	124	136
SRT277_2	-12	0	136	148
SRT278_2	-12	0	148	180
SRT279_2	-26	-13	-180	-124
SRT280_2	-26	-12	-78	-62
SRT281_2	-26	-12	-62	-50
SRT282_2	-26	-12	-50	-37
SRT283_2	-26	-12	-30	24
SRT284_2	-26	-12	24	36
SRT285_2	-26	-12	36	64
SRT286_2	-26	-12	96	126
SRT287_2	-26	-12	126	138
SRT288_2	-26	-12	138	150
SRT289_2	-26	-12	150	180
SRT290_2	-56	-26	-179	-70
SRT291_2	-56	-26	-70	-63
SRT292_2	-56	-26	-63	-34
SRT293_2	-55	-26	-13	78
SRT294_2	-36	-26	113	134
SRT295_2	-44	-26	134	147
SRT296_2	-56	-26	147	180

Annex C Mission Planner Report Example

The Plan Future Acquisition tool generates a Microsoft Word report describing the case evaluated and the appropriate acquisition parameters for future missions. This annex shows a report example.

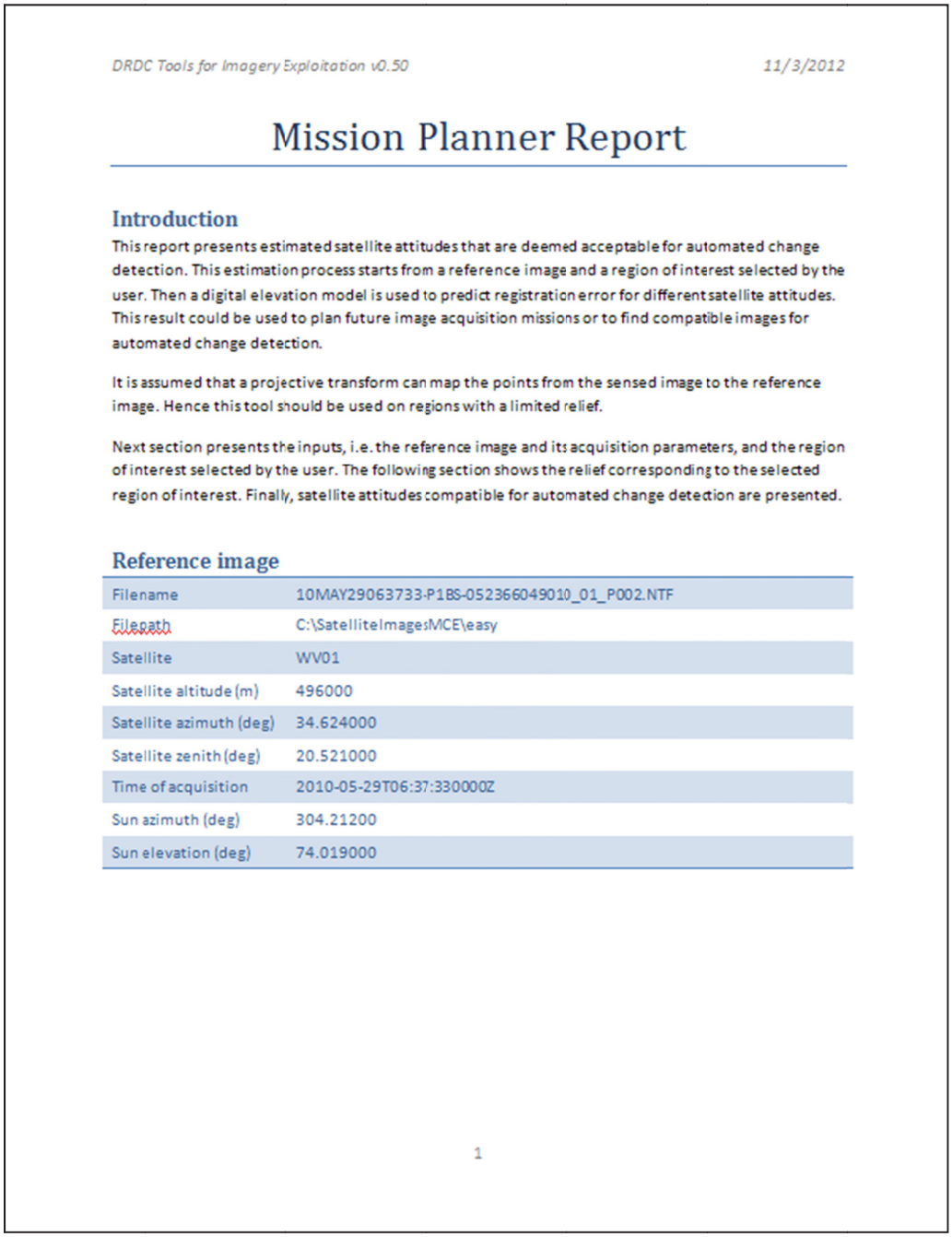

DRDC Tools for Imagery Exploitation v0.50 *11/3/2012*

Mission Planner Report

Introduction

This report presents estimated satellite attitudes that are deemed acceptable for automated change detection. This estimation process starts from a reference image and a region of interest selected by the user. Then a digital elevation model is used to predict registration error for different satellite attitudes. This result could be used to plan future image acquisition missions or to find compatible images for automated change detection.

It is assumed that a projective transform can map the points from the sensed image to the reference image. Hence this tool should be used on regions with a limited relief.

Next section presents the inputs, i.e. the reference image and its acquisition parameters, and the region of interest selected by the user. The following section shows the relief corresponding to the selected region of interest. Finally, satellite attitudes compatible for automated change detection are presented.

Reference image

Filename	10MAY29063733-P1BS-052366049010_01_P002.NTF
Filepath	C:\SatelliteImagesMCE\easy
Satellite	WV01
Satellite altitude (m)	496000
Satellite azimuth (deg)	34.624000
Satellite zenith (deg)	20.521000
Time of acquisition	2010-05-29T06:37:330000Z
Sun azimuth (deg)	304.21200
Sun elevation (deg)	74.019000

1

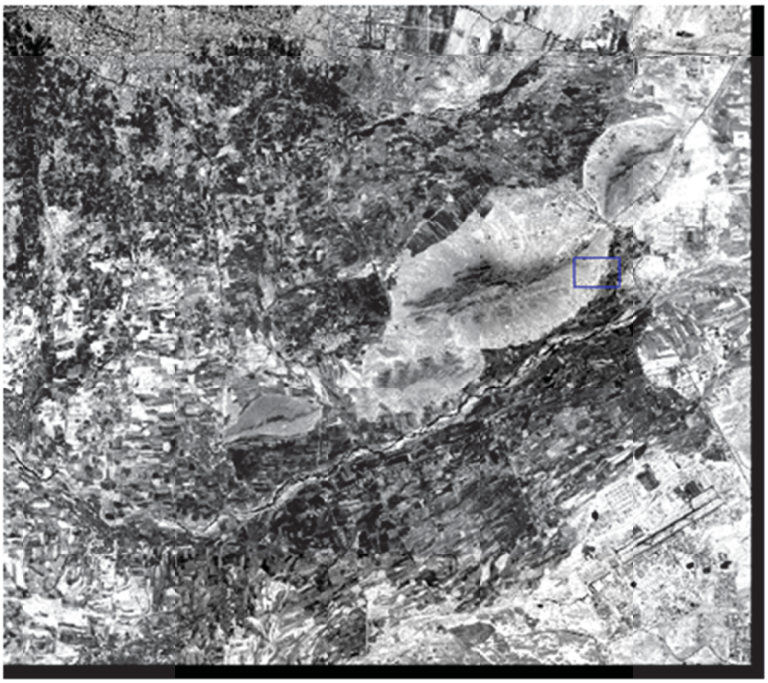

Figure 1: Reference image with regions of interest (blue)

Figure 2: Region of interest

Digital elevation model

Filename	n31.dt2
Filepath	C:\Projects\ImSpectrales\phase2\spectralimages\dted\data\dt2\e065
Resolution (m)	26
Min (m)	1016
Max (m)	1172
Average (m)	1033.88
Standard deviation (m)	27.6325

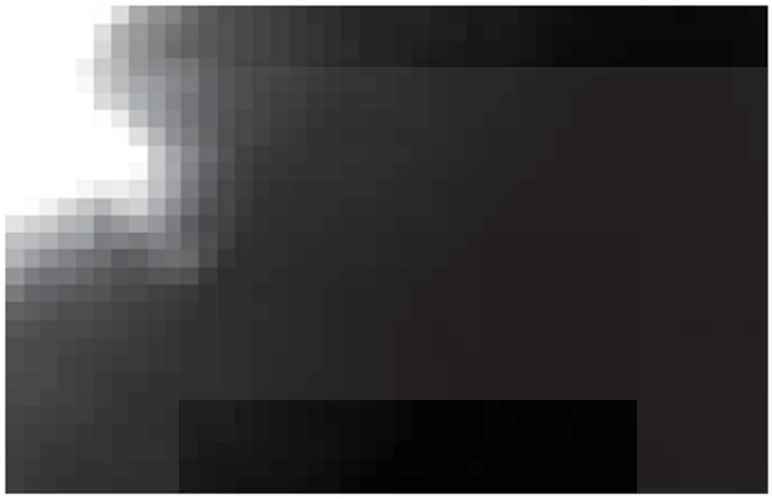

Figure 3: Digital elevation model of region of interest

Figure 4: Digital elevation model of region of interest - Slopes

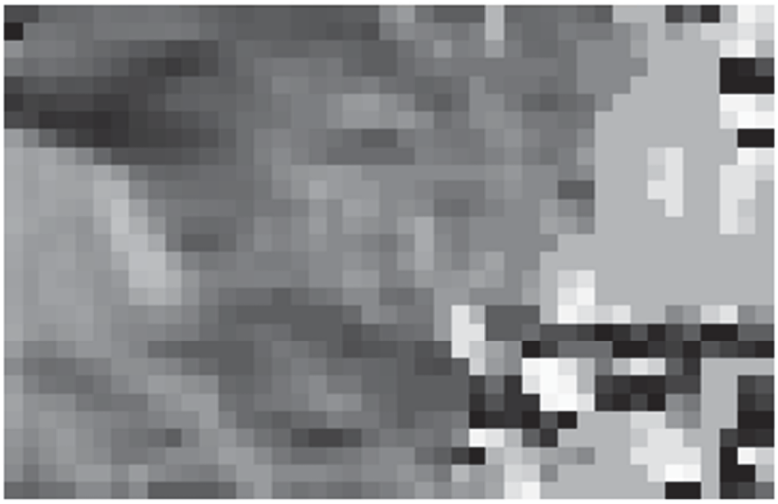

Figure 5: Digital elevation model of region of interest - Aspects

Valid acquisition parameters

Figure 4 shows the satellite attitudes for which the registration error was estimated. The green Xs show the parameters allowing a good performance of the automated change detection algorithms. The yellow Xs are for the parameters that will give an average performance for change detection, meaning many false alarms. In red are the parameters deemed intractable.

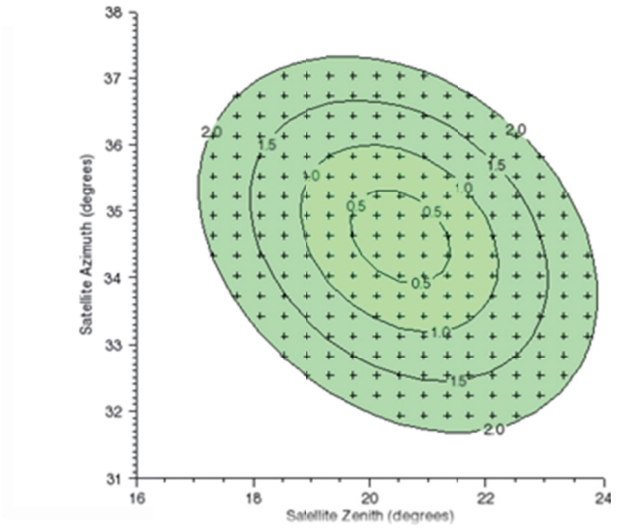

Figure 6: Valid satellite attitudes for future acquisitions

Figure 5 shows the estimated registration error for a varying zenith and a fixed azimuth of 0, i.e. the same azimuth as the reference image. The green and yellow lines show respectively the threshold for good and average change detection performance.

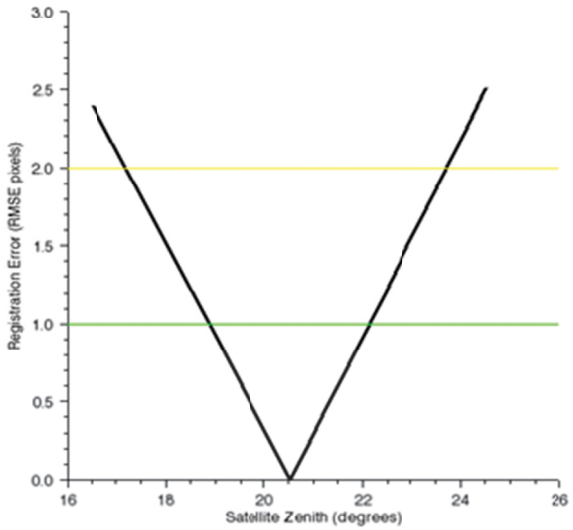

Figure 7: Estimation registration error for satellite azimuth 0

This page intentionally left blank.

List of symbols/abbreviations/acronyms/initialisms

ACE	Adaptive Coherence Estimator
ArcGIS	Arc Geographic Information System
BRDF	bidirectional reflectance distribution function
CDF	Cumulative Distribution Function
CEM	Constrained Energy Minimization
DEM	Digital Elevation Model
DMP	Differential Morphological Profile
DRDC	Defence Research and Development Canada
DTIE	DRDC Tools for Imagery Exploitation
FL	François Leduc
GSD	Ground Sampling Distance
IDL	Interactive Data Language
KAF	Kandahar Air Field
MP	Morphological Profile
NIFT	National Imagery Transmission Format
PWGSC	Publics Works Government Services Canada
RANSAC	Random Sample Consensus
RDDC	Recherche et développement pour la défence Canada
ROI	Region of Interest
SIFT	Scale-invariant feature transform
XROI	X Region of Interest (IDL tool)

This page intentionally left blank.

DOCUMENT CONTROL DATA

(Security markings for the title, abstract and indexing annotation must be entered when the document is Classified or Designated)

1. ORIGINATOR (The name and address of the organization preparing the document. Organizations for whom the document was prepared, e.g. Centre sponsoring a contractor's report, or tasking agency, are entered in section 8.)

AEREX Avionics Inc.
324, Saint-Augustin Avenue
Breakeyville (Québec) G0S IEI

2a. SECURITY MARKING (Overall security marking of the document including special supplemental markings if applicable.)

UNCLASSIFIED

2b. CONTROLLED GOODS

(NON-CONTROLLED GOODS)
DMC A
REVIEW: GCEC JUNE 2010

3. TITLE (The complete document title as indicated on the title page. Its classification should be indicated by the appropriate abbreviation (S, C or U) in parentheses after the title.)

DRDC Tools for Imagery Exploitation : Final Report

4. AUTHORS (last name, followed by initials – ranks, titles, etc. not to be used)

Labbé, V.

5. DATE OF PUBLICATION (Month and year of publication of document.)	6a. NO. OF PAGES (Total containing information, including Annexes, Appendices, etc.)	6b. NO. OF REFS (Total cited in document.)
March 2012	80	24

7. DESCRIPTIVE NOTES (The category of the document, e.g. technical report, technical note or memorandum. If appropriate, enter the type of report, e.g. interim, progress, summary, annual or final. Give the inclusive dates when a specific reporting period is covered.)

Contract Report

8. SPONSORING ACTIVITY (The name of the department project office or laboratory sponsoring the research and development – include address.)

Defence Research and Development Canada – Valcartier
2459 Pie-XI Blvd North
Quebec (Quebec)
G3J 1X5 Canada

9a. PROJECT OR GRANT NO. (If appropriate, the applicable research and development project or grant number under which the document was written. Please specify whether project or grant.)	9b. CONTRACT NO. (If appropriate, the applicable number under which the document was written.)
	W7701-092854/001/QCL

10a. ORIGINATOR'S DOCUMENT NUMBER (The official document number by which the document is identified by the originating activity. This number must be unique to this document.)	10b. OTHER DOCUMENT NO(s). (Any other numbers which may be assigned this document either by the originator or by the sponsor.)
2012-92854-1	DRDC Valcartier CR 2013-037

11. DOCUMENT AVAILABILITY (Any limitations on further dissemination of the document, other than those imposed by security classification.)

Unlimited

12. DOCUMENT ANNOUNCEMENT (Any limitation to the bibliographic announcement of this document. This will normally correspond to the Document Availability (11). However, where further distribution (beyond the audience specified in (11) is possible, a wider announcement audience may be selected.))

Unlimited

13. ABSTRACT (A brief and factual summary of the document. It may also appear elsewhere in the body of the document itself. It is highly desirable that the abstract of classified documents be unclassified. Each paragraph of the abstract shall begin with an indication of the security classification of the information in the paragraph (unless the document itself is unclassified) represented as (S), (C), (R), or (U). It is not necessary to include here abstracts in both official languages unless the text is bilingual.)

This document presents a suite of tools implementing the different steps toward automatic change detection on selected satellite images. These tools could be used by an image analyst to facilitate his work, and could also serve for designing an automated detection processing pipeline. This suite of tools is divided into three sets: 1) error prediction and images co-registration, 2) change detection, and 3) target detection. The suite was integrated into Excelis ENVI 4.7/IDL 7.1.1 but was also tested with ENVI 4.8.

Ce rapport présente un ensemble d'outils mettant en œuvre les étapes nécessaires à la détection automatique de changements sur un sous-ensemble d'images satellite sélectionnées. Ces outils peuvent assister un analyste dans son travail, ou pourraient être assemblés pour créer une chaîne de traitement automatique. Ces outils sont divisés en trois catégories: 1) prédiction de l'erreur de recalage et recalage d'images, 2) détection de changements et 3) détection de cibles. Cet ensemble d'outils est intégré à Excelis ENVI 4.7/IDL 7.1.1 mais a aussi testé avec ENVI 4.8.

14. KEYWORDS, DESCRIPTORS or IDENTIFIERS (Technically meaningful terms or short phrases that characterize a document and could be helpful in cataloguing the document. They should be selected so that no security classification is required. Identifiers, such as equipment model designation, trade name, military project code name, geographic location may also be included. If possible keywords should be selected from a published thesaurus, e.g. Thesaurus of Engineering and Scientific Terms (TEST) and that thesaurus identified. If it is not possible to select indexing terms which are Unclassified, the classification of each should be indicated as with the title.)

images coregistration; performance prediction; automatic change detection; target detection; SRT2 DTED geographic limits; target detection; Excelis ENVI 4.7/IDL 7.1.1

Defence R&D Canada

Canada's Leader in Defence
and National Security
Science and Technology

R & D pour la défense Canada

Chef de file au Canada en matière
de science et de technologie pour
la défense et la sécurité nationale

www.drdc-rddc.gc.ca